BIOCHEMISTRY
including biophysical chemistry & molecular biology

Article

pubs.acs.org/biochemistry

Thio Effects and an Unconventional Metal Ion Rescue in the Genomic Hepatitis Delta Virus Ribozyme

Pallavi Thaplyal,[†] Abir Ganguly,[‡] Barbara L. Golden,*[,§] Sharon Hammes-Schiffer,*[,‡] and Philip C. Bevilacqua*[,†]

[†]Department of Chemistry and Center for RNA Molecular Biology, The Pennsylvania State University, University Park, Pennsylvania 16802, United States

[‡]Department of Chemistry, University of Illinois at Urbana-Champaign, Urbana, Illinois 61801, United States

[§]Department of Biochemistry, Purdue University, West Lafayette, Indiana 47907, United States

Supporting Information

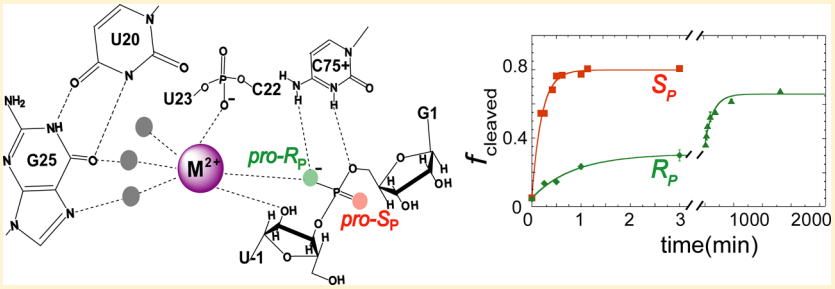

ABSTRACT: Metal ion and nucleobase catalysis are important for ribozyme mechanism, but the extent to which they cooperate is unclear. A crystal structure of the hepatitis delta virus (HDV) ribozyme suggested that the *pro*-R_P oxygen at the scissile phosphate directly coordinates a catalytic Mg^{2+} ion and is within hydrogen bonding distance of the amine of the general acid C75. Prior studies of the genomic HDV ribozyme, however, showed neither a thio effect nor metal ion rescue using Mn^{2+}. Here, we combine experiment and theory to explore phosphorothioate substitutions at the scissile phosphate. We report significant thio effects at the scissile phosphate and metal ion rescue with Cd^{2+}. Reaction profiles with an S_P-phosphorothioate substitution are indistinguishable from those of the unmodified substrate in the presence of Mg^{2+} or Cd^{2+}, supporting the idea that the *pro*-S_P oxygen does not coordinate metal ions. The R_P-phosphorothioate substitution, however, exhibits biphasic kinetics, with the fast-reacting phase displaying a thio effect of up to 5-fold and the slow-reacting phase displaying a thio effect of ∼1000-fold. Moreover, the fast- and slow-reacting phases give metal ion rescues in Cd^{2+} of up to 10- and 330-fold, respectively. The metal ion rescues are unconventional in that they arise from Cd^{2+} inhibiting the oxo substrate but not the R_P substrate. This metal ion rescue suggests a direct interaction of the catalytic metal ion with the *pro*-R_P oxygen, in line with experiments with the antigenomic HDV ribozyme. Experiments without divalent ions, with a double mutant that interferes with Mg^{2+} binding, or with C75 deleted suggest that the *pro*-R_P oxygen plays at most a redundant role in positioning C75. Quantum mechanical/molecular mechanical (QM/MM) studies indicate that the metal ion contributes to catalysis by interacting with both the *pro*-R_P oxygen and the nucleophilic 2′-hydroxyl, supporting the experimental findings.

The hepatitis delta virus (HDV) ribozyme is a small ∼85-nucleotide RNA that occurs in closely related genomic and antigenomic forms and is important in the life cycle of the virus.[1,2] It self-cleaves at the phosphodiester bond between U−1 and G1 to generate products with 2′,3′-cyclic phosphate and 5′- hydroxyl termini. The secondary structure has five pairings, P1−P4 and P1.1, which comprise two pseudoknots that provide a compact fold (Figure 1A).[3,4] The ribozyme has several conserved residues, including the catalytic C75, which participates in proton transfer, and one standard and one reverse G·U wobble (Figure 1).[5,6] The HDV ribozyme is unique among the well-characterized ribozymes in its ability to employ both nucleobase and metal ion catalysis in its reaction mechanism.[7]

Several studies support C75 as the general acid in the reaction. Early experiments indicated that removal of this C can be rescued by the addition of imidazole,[8] indicating a role in proton transfer, which was supported by Brønsted studies.[9,10] Solution kinetic studies revealed a shift of the pK_a for C75 by 2−3 units toward neutrality and an inverted rate−pH profile in the absence of Mg^{2+}.[11−13] Direct measurements of the pK_a shifted toward neutrality were accomplished using Raman studies on crystals of a precleaved genomic ribozyme.[14] Importantly, substitution of 5′-phosphorothiolate at the scissile phosphate resulted in a hyperactive 5′-leaving group that was readily cleaved by the C75U mutant, strongly implicating C75 as the general acid.[15]

Received: January 17, 2013
Revised: June 11, 2013
Published: September 3, 2013

dx.doi.org/10.1021/bi4000673 | *Biochemistry* 2013, 52, 6499−6514

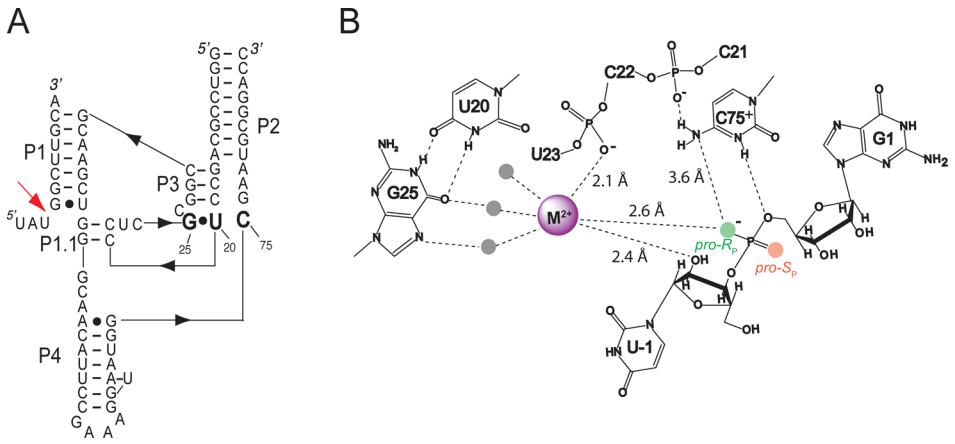

Figure 1. Secondary structure and active site interactions in the genomic HDV ribozyme. (A) Secondary structure of the *trans*-cleaving HDV ribozyme studied herein. The ribozyme consists of an enzyme strand and a substrate, which comprises the cleavage site shown by the red arrow. The catalytic nucleobase C75 and the reverse wobble G25·U20, important in metal ion binding, are depicted in bold. In addition, there is a standard wobble G1·U37 at the cleavage site. The construct shown here is in a fast-reacting background[79] and has a shortened P4, as used in crystallography of the precleaved state;[5] the original numbering of the 3′-portion is maintained. (B) Active site of the HDV ribozyme depicting catalytically important residues according to a precleaved crystal structure.[5] The *pro*-R_P oxygen (green) is positioned near the catalytic metal ion (2.6 Å) and the amine of C75 (3.6 Å), which in turn interacts with the phosphate of C22. The active site Mg^{2+} has three direct interactions: with the 2′-OH of U-1, the *pro*-R_P oxygen of the scissile phosphate, and the phosphate of U23. In addition, this Mg^{2+} ion interacts with the reverse G·U wobble through its hydration shell. The distances are according to ref 5.

Structural studies of these crystals revealed that C75 is positioned to protonate the leaving group, 5′-O of G1.[3,5] Furthermore, both pH−rate profiles and pH-dependent Raman crystallography revealed anticooperative interaction between protonated C75 and Mg^{2+}, suggesting an important relationship between nucleobase and metal ion catalysis in the reaction mechanism.[11,14]

Metal ions can contribute to RNA catalysis through specific and nonspecific modes of action.[16,17] With the HDV ribozyme in particular, a wide range of divalent ions contribute to catalysis, including most alkaline earth and certain transition metals.[18,19] According to a multichannel framework for the genomic ribozyme, divalent metal ions contribute 3000-fold to the reaction: ∼125-fold to folding and ∼25-fold to catalysis.[12] In addition, the genomic HDV ribozyme is partially active in the absence of divalent metal ions: a study of the genomic and antigenomic HDV ribozymes in monovalent ions found that a high concentration of monovalent ions was required to compensate for the absence of divalent metal ions.[20]

A recently determined crystal structure of the precleaved HDV ribozyme reveals that the catalytic metal ion is positioned, in part, by water-mediated interactions with a rare but absolutely conserved reverse G·U wobble (Figure 1B).[5] However, the cleavage site was partially disordered, which necessitated modeling in this portion of the structure. It is therefore critical to test the proposed metal ion interactions using mechanistic biochemical studies. Recent characterization of a mutant that replaces the reverse G·U wobble with a reverse A·C wobble functionally links the metal ion observed in the crystal structure with the catalytic metal ion.[6] According to the crystal structure, this metal ion is positioned with the help of the *pro*-R_P oxygen of the scissile phosphate and the phosphate group of U23. These interactions allowed a model to be built in which the metal ion coordinates the nucleophile in the reaction, the 2′-O of U−1. Thus, the metal ion could potentially play a dual role in catalysis: a Lewis acid to facilitate deprotonation of the nucleophile and a Brønsted base to accept the proton from the nucleophile. A goal of this study is to test structural features of that model using mechanistic studies.

Here, we characterize the network of interactions involving the *pro*-R_P oxygen of the scissile phosphate. A previous analysis of sulfur substitutions at the scissile phosphate of the genomic HDV ribozyme suggested the potential functional importance of the *pro*-R_P oxygen, as cleavage reactions in the presence of an R_P sulfur substitution did not proceed to completion.[21] However, those studies did not reveal a thio effect or a metal ion rescue by Mn^{2+}, the only thiophilic metal ion used to attempt rescue.[21,22] Those studies may have been hampered by the strong propensity of the genomic HDV ribozyme to misfold.[23] In contrast to these results, the crystal structure of the precleaved HDV ribozyme did implicate the *pro*-R_P oxygen in a direct interaction with the putative catalytic metal ion (Figure 1B).[5] The ribozyme construct used to determine this structure is a variant of a ribozyme developed in our laboratories, which is especially fast-reacting and folds homogeneously into its native structure.[23] Extensive characterization of this variant demonstrates that it has a rate-limiting step of bond cleavage, supported by solvent isotope effects, proton inventories, theoretical studies, and a pK_a shifted toward neutrality that is in agreement with Raman crystallographic studies.[11,24−27] We therefore used this variant to examine the thio effect at the scissile phosphate and to fully characterize the metal ion rescue with a wider array of thiophilic metal ions.

MATERIALS AND METHODS

RNA Oligonucleotides and Constructs. The RNA was prepared in two pieces. The first strand, formally the enzyme, spans 64 nucleotides (Figure 1A) and was prepared by T7 transcription under standard conditions as previously described.[5] The sequence was cloned into pUC19 and confirmed using dideoxy sequencing. The same procedure was used for the transcription of the G25A·U20C double-mutant ribozyme, where the reverse G25·U20 wobble was mutated to a reverse A·C wobble.[6] For the C75Δ ribozyme, the enzyme strand was transcribed using T7 RNA polymerase from a hemiduplex consisting of the top strand with a 5′ TAA TAC GAC TCA CTA

dx.doi.org/10.1021/bi4000673 | *Biochemistry* 2013, 52, 6499−6514

TA sequence and the bottom strand containing a 5′ GGT CCG CAT TCC CAT TAC CTT TCG GAA TGT TGC CCA GCT TGC GCC GCG AGG AGG CTG CGG ACC TAT AGT GAG TCG TAT TA sequence.

Following transcription, the enzyme pieces were purified on an 8% polyacrylamide−7 M urea gel. Bands were visualized by UV shadowing and excised from the gel. RNA was eluted overnight at 4 °C into 10 mM Tris-HCl, 0.1 mM EDTA, and 250 mM NaCl, precipitated with 3 volumes of ethanol, and stored at −20 °C.

The second strand, formally the substrate, spans the 5′-strand of P1 and its upstream region and contains the cleavage site. This strand was prepared by solid-phase synthesis (Dharmacon Inc.). The sequence of the substrate is 5′ UAU*GGCUUGCA, where the asterisk denotes the site of cleavage and phosphorothioate substitution. A synthetic oligonucleotide containing the single phosphorothioate substitution was separated into the S_P and R_P diastereomers by C18 reverse-phase high-performance liquid chromatography (HPLC) (solvent A, 0.1 M NH_4OAc; solvent B, 50% solvent A and 50% CH_3CN) starting with solvent A and employing a linear gradient (0 to 15% over 45 min, followed by 10 min more at 15%) of solvent B. The R_P and S_P isomers were well-resolved, as confirmed by reinjecting the purified material into the HPLC instrument (Figure S1 of the Supporting Information). The R_P isomer elutes first from the column, as described previously.[21] The identities of the R_P and S_P isomers were confirmed with snake venom phosphodiesterase (data not shown). Purified fractions were dried, redissolved in sterile water, and stored at −20 °C. The separated diastereomers were reanalyzed by HPLC regularly (on an approximately bimonthly basis), which confirmed absence of contamination, desulfurization of the stock solutions, and degradation. Furthermore, the oxo, R_P and S_P substrates were subjected to iodine (1 mM) cleavage at 90 °C for 2 min in the absence of enzyme or after various incubations in the presence of the enzyme.[28,29] The iodine was found to cleave the R_P and S_P substrates to the same extent with and without enzyme (Figure S2 of the Supporting Information), which showed that both substrates contained sulfur and were not being desulfurized throughout the course of the reaction. Purified oligonucleotides were treated with T4 polynucleotide kinase (New England Biolabs) and [γ-^{32}P]ATP to add a radiolabeled phosphate to their 5′-ends prior to kinetic analysis.

In-Line Probing. In-line probing (ILP) experiments were conducted in a manner similar to that previously described.[30] Briefly, the transcribed enzyme strand was treated with calf intestine phosphatase and then with T4 polynucleotide kinase and [γ-^{32}P]ATP to add a radiolabeled phosphate to its 5′-end. Next, 2 μL of labeled HDV enzyme strand (∼2 nM) and 2 μL of substrate (∼2 μM) were heated at 90 °C and then cooled at room temperature for 5 min. Substrate was in excess to ensure that the enzyme strand was present in the substrate-bound state. Following this, 2× in-line probing buffer [1× in-line probing buffer consists of 50 mM Tris-HCl (pH 8.3), 20 mM Mg^{2+}, and 100 mM KCl] was added to reach a total volume of 20 μL. A control ILP reaction was performed in the absence of the substrate strand. Reaction mixtures were incubated at 37 °C, and 5 μL time points were taken at 5 min, 20 h, and 40 h and quenched with an equal volume of 2× formamide loading buffer [1x formamide loading buffer consists of 50 mM EDTA, 50 mM Tris-HCl (pH 8.3), formamide, and loading dyes] and immediately placed on dry ice. An RNase T1 ladder was generated by heating the enzyme strand with 0.05 unit of RNase T1 at 50 °C for 5 min and then quenching on dry ice, and a hydrolysis ladder was generated by heating the 5′-end-labeled enzyme strand with 50 mM sodium carbonate (pH 9.2) and 1 mM EDTA at 95 °C for 2 min. Samples were fractionated on an 8% denaturing polyacrylamide gel electrophoresis gel.

Kinetic Assays and Data Analysis. All reactions were single-turnover and performed at 37 °C. $CdCl_2$*2.5(H_2O) was purchased from Sigma Aldrich (>98% purity). Similar results were obtained with anhydrous $CdCl_2$ from Sigma Aldrich (>99% purity). To avoid precipitation of Cd^{2+} as $Cd(OH)_2$, a 100 mM $CdCl_2$ stock solution was prepared in NaMES (12.5 mM, pH 5.6) and subsequently diluted. The ribozyme (3 μM) was annealed to trace amounts of end-labeled substrate (<2 nM) at 90 °C for 2 min and then cooled at room temperature for 10 min followed by the addition of either NaMES (25 mM, pH 5.6) or NaHEPES (25 mM, pH 8.0). To confirm that all of the substrate is bound, we performed the reactions with an increasing enzyme concentration of up to 16 μM under the conditions described above. Increasing the enzyme concentration above 3 μM did not affect the observed reaction rate, confirming that 3 μM ribozyme was sufficient to bind all the substrate.

The reaction was initiated by adding a pre-equilibrated metal ion mix to the other reaction components that led to final Mg^{2+} concentrations of 10 or 50 mM with 0−10 mM Cd^{2+}. At regular intervals, 3 μL aliquots were removed, quenched via addition to an equal volume of a 96% formamide/20 mM EDTA mixture, and placed immediately on powdered dry ice. The efficacy of the quench was confirmed by adding the quench prior to the addition of divalent metal ion and observing absence of reaction. Quench efficacy was confirmed under a number of reaction conditions: 10 mM Mg^{2+} (pH 5.6 and 8.0), 10 mM Mg^{2+} with 10 mM Cd^{2+} (pH 5.6), and 10 mM Mg^{2+} with 2 mM Cd^{2+} (pH 8.0). The AC double-mutant reactions were performed similarly, with a final ribozyme concentration of 5 μM to provide direct comparison with our previous study.[6]

For the C75Δ reaction, trace amounts of the labeled substrate (<2 nM) and 3 μM ribozyme were heated at 90 °C for 2 min, allowed to cool to room temperature, and then incubated at 37 °C for 10 min in 5 mM Tris-HCl (pH 7.5) and 0.1 M NaCl. The renatured RNA was then diluted in reaction buffer to final concentrations of 25 mM $MgCl_2$, 0.5 mM spermidine, and 0.4 M imidazole (pH 7.0), as per earlier studies of C75Δ.[10] Aliquots were removed at regular intervals, quenched with an equal volume of a high-EDTA quench of 90% formamide/50 mM EDTA mixture, and placed immediately on powdered dry ice. Control reactions of the C75Δ ribozyme conducted in the absence of imidazole showed no reaction. Reactions with WT ribozyme in the absence of divalent metal ions were performed as previously described.[26]

For all reactions, the 5′-end-labeled cleavage product was separated on 16% acrylamide−7 M urea gels, and the fraction of the substrate cleaved versus time was quantified using a Typhoon PhosphorImager (Molecular Dynamics). Data from the oxo and S_P substrate were fit to a single-exponential equation:

$$f_{\text{cleaved}} = A + Be^{-k_{\text{obs}}t} \quad (1)$$

where f_{cleaved} is the fraction of substrate cleaved, k_{obs} is the observed first-order rate constant, A is the fraction of the ribozyme cleaved at completion, $-B$ is the amplitude of the observable phase, $1 - A$ is the unreactive fraction, and $A + B$ is the amplitude of the burst fraction, which was ∼0 herein.

Data from the R_P substrate were fit to a double-exponential equation:

dx.doi.org/10.1021/bi4000673 | Biochemistry 2013, 52, 6499−6514

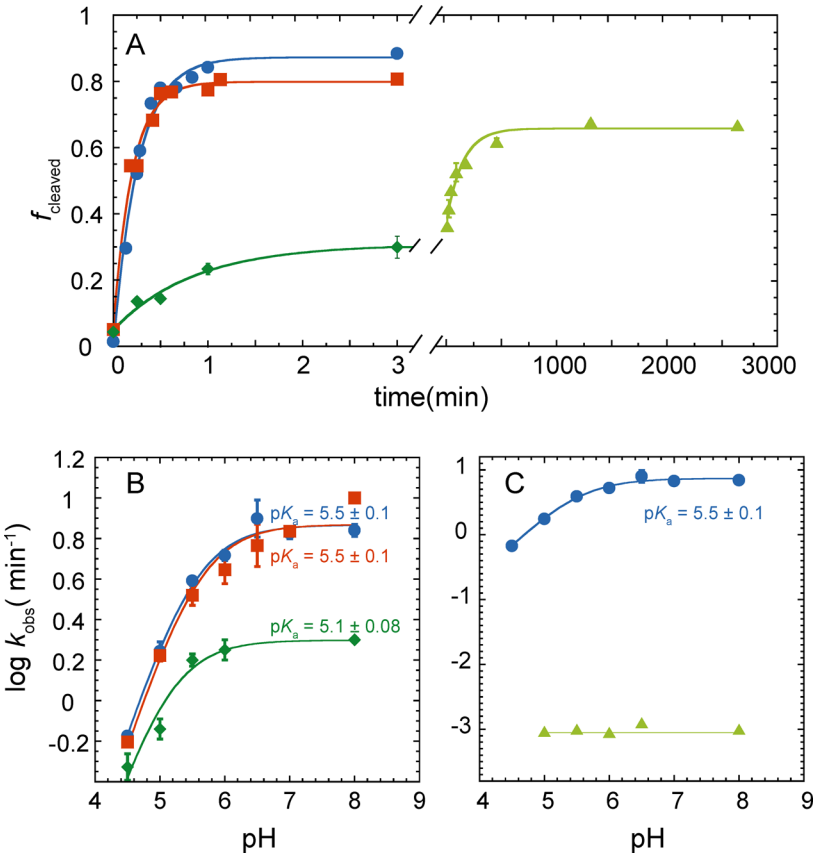

Figure 2. R_P substrate has substantial thio effects and a perturbed pK_a. (A) Fraction cleaved vs time traces of the oxo (blue circles), S_P (red squares), R_P fast phase (dark green diamonds), and R_P slow phase (light green triangles) at pH 5.6 (same colors and shapes used in all graphs). Traces were fit to eq 1 for the oxo and S_P substrates and to eq 2 for the R_P substrate. The oxo and S_P substrates react monophasically and close to completion, with k_{obs} values of 4.1 ± 0.2 and 4.4 ± 0.2 min^{-1}, respectively. The R_P substrate, on the other hand, reacts biphasically, and both phases react slower than the oxo substrate, which constitutes thio effects. The fast and slow R_P phases react ~3-fold (k_{obs} = 1.5 ± 0.8 min^{-1}) and ~1000-fold (k_{obs} = 0.004 ± 0.001 min^{-1}) slower than the oxo substrate. (B) pH−rate profiles of the oxo, S_P, and R_P fast-reacting substrates. The pK_a of C75 when the substrate is oxo or S_P was found to be ~5.5 ± 0.1, while the pK_a of C75 when the substrate is the R_P fast substrate was 5.1 ± 0.08. (C) pH−rate profile of the oxo substrate shown in comparison to that of the slow-reacting R_P substrate, which is independent of pH over this range. All data are in a background of 10 mM Mg^{2+}.

$$f_{cleaved} = A + Be^{-k_1 t} + Ce^{-k_2 t} \quad (2)$$

where k_1 and k_2 are the observed first-order rate constants for the fast and slow phases, respectively, A is the fraction of the ribozyme cleaved at completion, $-B$ and $-C$ are the amplitudes of the observable phases, $1 - A$ is the unreactive fraction, and $A + B + C$ is the amplitude of the burst fraction, which was ~0 herein. The error is reported as the standard deviation of two or more measurements.

For slower reactions, time courses were followed for up to several days; control experiments from which the enzyme was omitted showed that the cleaved product obtained was not from substrate degradation. In particular, at time points of 60 h in a 1 M NaCl/100 mM EDTA mixture and 20 h in a C75Δ/25 mM Mg^{2+} mixture, the oxo and R_P substrates showed only ~5 and ~2% degradation, respectively, while the actual reaction typically had undergone ~15−20% reaction at these time points.

Calculations of the Thio Effect and Metal Ion Rescue. Substitution of the nonbridging oxygen with sulfur alters the observed ribozyme kinetics by a factor noted as the "thio effect", which is defined as follows:[31,32]

$$\text{thio effect} = \left(\frac{k_O}{k_S}\right)^{Mg^{2+}} \quad (3)$$

where k_O is the k_{obs} for the oxo substrate and k_S is the k_{obs} for the phosphorothioate substrate. Because the thio effect is defined in the absence of thiophilic metal ion but in the presence of Mg^{2+}, we add a superscript Mg^{2+} to the equation. A normal thio effect is defined as a thio effect greater than unity, while an inverse thio effect is less than unity.

Rescue of a thio effect greater than unity by a thiophilic metal ion (denoted as M^{2+}) is defined as "metal ion rescue". In general, addition of a thiophilic metal ion, typically in a background of Mg^{2+} to aid native ribozyme folding, may affect the rate of the wild-type reaction, too, for example, by competing with Mg^{2+} for an ion site or through an allosteric effect. To account for this, metal ion rescue is generally defined as the ratio of k_S in the presence of M^{2+} to k_S in the presence of Mg^{2+} only, normalized to this ratio for the all-oxo substrate (k_O):[33]

$$\text{metal ion rescue} = \left(\frac{{k_S}^{M^{2+}}}{{k_S}^{Mg^{2+}}}\right) \Big/ \left(\frac{{k_O}^{M^{2+}}}{{k_O}^{Mg^{2+}}}\right) = \left(\frac{k_O}{k_S}\right)^{Mg^{2+}} \Big/ \left(\frac{k_O}{k_S}\right)^{M^{2+}} \quad (4)$$

A mathematically equivalent ratio of ratios is provided on the second line of eq 4, which considers the thio effect, $(k_O/k_S)^{Mg^{2+}}$,

dx.doi.org/10.1021/bi4000673 | Biochemistry 2013, 52, 6499−6514

Table 1. Thio Effect and Metal Ion Rescue for the HDV Ribozyme in the Presence of 10 mM Mg^{2+} at pH 5.6 and 8.0[a]

ionic conditions	substrate	k_{obs} (min^{-1})[b]	end point (%)	k_O/k_S[c]	metal ion rescue[d]
		pH 5.6 Conditions			
10 mM Mg^{2+}	oxo	4.1 ± 0.2	90 ± 1	N/A[f]	N/A[f]
	S_P	4.4 ± 0.2	81 ± 2	0.93 ± 0.07	
	R_P fast	1.5 ± 0.8	28 ± 10	2.8 ± 1.4	
	R_P slow	0.004 ± 0.001	43 ± 10	(1.0 ± 0.25) × 10^3	
10 mM Mg^{2+} with 2 mM Cd^{2+}	oxo	0.17 ± 0.07	84 ± 4	N/A[f]	N/A[f]
	S_P	0.09 ± 0.02	79 ± 4	2 ± 0.9	0.5 ± 0.2
	R_P fast	0.4 ± 0.2	11 ± 4	0.4 ± 0.2	7.5 ± 4.3
	R_P slow	0.003 ± 0.0007	39 ± 1	57 ± 27	18 ± 9.6
10 mM Mg^{2+} with 10 mM Cd^{2+}	oxo	0.006 ± 0.0001	74 ± 1	N/A[f]	N/A[f]
	S_P	0.004 ± 0.0001	50 ± 4	1.5 ± 0.06	0.5 ± 0.1
	R_P slow[e]	0.002	42	3.0 ± 0.05	(3.33 ± 1.0) × 10^2
10 mM Mg^{2+} with 2 mM Mn^{2+}	oxo	3.7 ± 0.1	73 ± 1	N/A[f]	N/A[f]
	S_P	4.0 ± 0.5	70 ± 2	0.92 ± 0.12	1.0 ± 0.15
	R_P fast	0.78	6	4.77 ± 0.15	0.6 ± 0.15
	R_P slow	0.001	43	(3.70 ± 0.15) × 10^3	0.3 ± 0.02
		pH 8.0 Conditions			
10 mM Mg^{2+}	oxo	7.0 ± 0.5	81 ± 1	N/A[f]	N/A[f]
	S_P	8.0 ± 1.6	70 ± 10	0.87 ± 0.2	
	R_P fast	1.45 ± 0.45	18 ± 1	4.8 ± 1.5	
	R_P slow	0.009 ± 0.001	32 ± 12	(7.7 ± 1.0) × 10^2	
10 mM Mg^{2+} with 0.5 mM Cd^{2+}	oxo	0.1 ± 0.001	68 ± 15	N/A[f]	N/A[f]
	S_P	0.03	65	3.0 ± 0.3	0.3 ± 0.07
	R_P fast	0.20 ± 0.01	9 ± 1	0.50 ± 0.06	10 ± 3.2
	R_P slow	0.004 ± 0.001	48 ± 1	25 ± 6.5	31 ± 8.9

[a] k_{obs} measured in the background of 10 mM Mg^{2+} at 37 °C and pH 5.6 (50 mM NaMES) or pH 8.0 (50 mM NaHEPES). [b] The error in k_{obs} is from the standard deviation of two or more experimental observations. [c] The thio effect is the k_O/k_S ratio at 10 mM Mg^{2+} in the absence of thiophilic metal ions (eq 3). The error is propagated from the relative errors.[34] [d] The metal ion rescue for each substrate is calculated as described in eq 4. [e] At 10 mM Cd^{2+}, the R_P substrate did not exhibit a biphasic behavior. We designated this R_P substrate as the "R_P slow phase" rather than "R_P fast phase" because the observed rates for this substrate are close to those of the R_P slow phase. Also, with increasing concentrations of Cd^{2+}, the amplitude of the R_P fast phase decreases. [f] Not applicable.

divided by the ameliorated thio effect in the presence of M^{2+}, $(k_O/k_S)^{Mg^{2+}}$. Error was propagated from the relative error by standard means.[34] Because eq 4 involves four rate constants, the error was larger, but still tolerable, for metal ion rescue.

Calculation of the Cd^{2+} Inhibition Constant. The competition between Cd^{2+} and Mg^{2+} was evaluated by a Dixon plot[35] in which the reciprocal of k_{obs} was plotted versus the concentration of Cd^{2+}, parametric in Mg^{2+} concentration. Intersection of these lines in the second quadrant is consistent with competitive interaction between the two ions, and the negative of the abscissa, corresponding to their point of intersection, provides an apparent K_i for Cd^{2+} binding.

Molecular Dynamics (MD) Simulations. The MD simulations were performed using DESMOND[36,37] with the AMBER99 force field.[38,39] Starting from the crystal coordinates, we obtained the *pro*-R_P sulfur and *pro*-S_P sulfur starting structures by mutating the corresponding oxygen atoms in the WT to sulfur *in silico*. C75 and C41 were kept in the active protonated state during all simulations. Details regarding the building of the simulation box and the equilibration procedure have been discussed previously.[40] In this study, two independent 25 ns trajectories were run for both the R_P and S_P cases.

Quantum Mechanical/Molecular Mechanical (QM/MM) Calculations. The QM/MM calculations are based on the precleaved HDV ribozyme coordinates (Protein Data Bank entry 3NKB).[5] The U-1 region was modeled into the 3NKB coordinates as previously described.[5] Hydrogen atoms were added to the entire ribozyme using Accelrys Discover Studio Visualizer version 2.0. Residues C41 and C75 were kept protonated at N3 during all calculations to provide structural stability and prepare C75 in its general acid functional form.[14,41] All 11 crystallographically resolved Mg^{2+} ions were included, and the ribozyme was immersed in rigid TIP3P water in a periodically replicated orthorhombic box. Counterions were added to neutralize the system, and 0.15 M NaCl was added to replicate the physiological ionic strength.

Starting configurations for the QM/MM calculations were obtained after MD equilibration of the solvent and ions, the protocol of which has been detailed elsewhere.[42] The MD simulations were performed with DESMOND[43] using the AMBER99 force field.[38] The QM/MM calculations were performed using QSite.[44] The QM region considered in this study is similar to that used in our previous study and included the sulfur and Cd atoms.[27] The QM region was treated with density functional theory at the B3LYP/6-31G**[45] level of theory using an ultrafine grid. The LACVP*[46,47] pseudopotential was used for the Cd^{2+} metal ion, and the hydrogen capping method was used for the residues at the QM region boundary. The MM region was described using the OPLS2005[48] force field, and the residue-based nonbonded cutoff was set to 100 Å. All atoms lying outside a radius of 20 Å from the scissile phosphate were held fixed throughout the QM/MM calculations. Each nonbridging oxygen of the scissile phosphate was replaced *in silico* with sulfur to obtain the corresponding R_P or S_P phosphorothioate diastereomer.

dx.doi.org/10.1021/bi4000673 | *Biochemistry* 2013, 52, 6499−6514

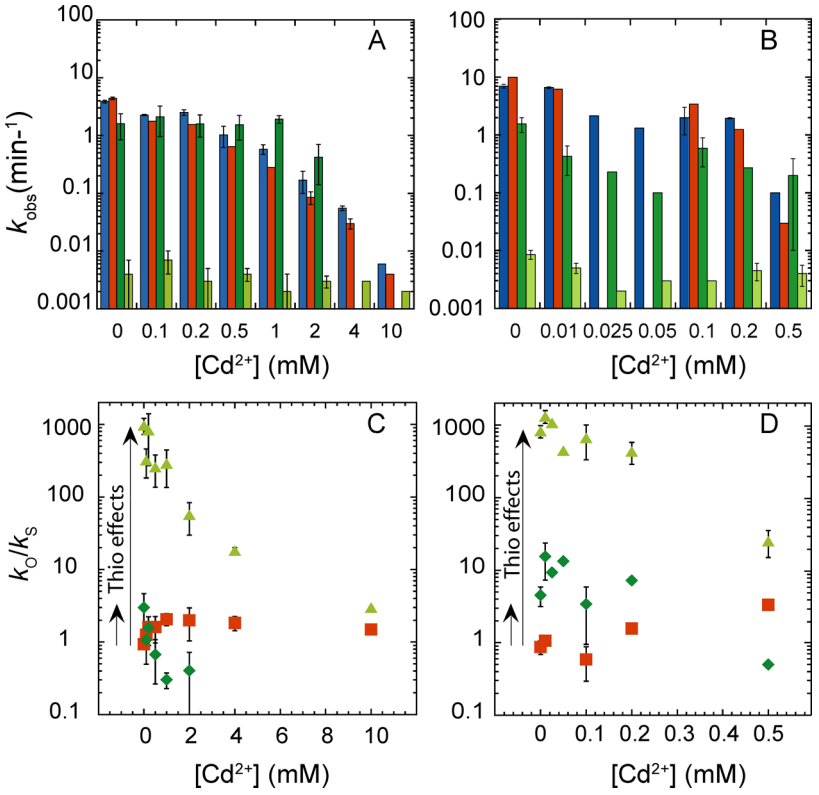

Figure 3. Dependence of k_{obs} and k_O/k_S on Cd^{2+} concentration. (A and B) Histograms representing k_{obs} values for the oxo (blue), S_P (red), R_P fast-phase (dark green), and R_P slow-phase (light green) substrates as a function of Cd^{2+} concentration at (A) pH 5.6 and (B) pH 8.0. (C and D) k_O/k_S values for the S_P (red squares), R_P fast-phase (dark green diamonds), and R_P slow-phase (light green triangles) substrates as a function of Cd^{2+} concentration at (C) pH 5.6 and (D) pH 8.0. Note that there is only a single phase (light green triangles) for the R_P substrate at Cd^{2+} concentrations of >2 mM. Note that data for the S_P substrate were not collected at 0.025 and 0.05 mM Cd^{2+} at pH 8.0. All data are in a background of 10 mM Mg^{2+}. The thio effects in the absence of Cd^{2+} for the R_P substrate fast- and slow-phases are represented by the short and long arrows, respectively.

RESULTS

Phosphorothioate Substitution Reveals a Thio Effect for the R_P Substrate. We began by examining the effects of sulfur substitution at each of the diastereotopic nonbridging oxygens of the scissile phosphate. These experiments were conducted with a fast-reacting variant of the genomic HDV ribozyme, which has chemistry as the rate-limiting step.[13,18,21,26] Single-turnover kinetic profiles with the oxo substrate in the presence of 10 mM Mg^{2+} were monophasic and went nearly to completion (Figure 2A). The rate−pH profile showed an increase in rate with pH followed by a plateau region (Figure 2B), similar to results previously described.[11] The apparent pK_a for the reaction with the oxo substrate was 5.5 ± 0.1, which is in reasonable agreement with the previously reported value of 6.1 ± 0.1.[a,11] The S_P substrate reacted monophasically with a nearly identical kinetic profile, rate−pH profile, and pK_a value (Figure 2A,B). This suggests that the S_P oxygen does not contribute significantly to the reaction, consistent with the crystal structure.

The R_P substrate, in contrast, reacted with a biphasic kinetic profile, with each phase showing a thio effect (Figure 2A). The rate for the fast phase of the R_P substrate increased with pH followed by a plateau and gave a pK_a of 5.1 ± 0.08 (Figure 2B). This value for the pK_a is somewhat smaller than that observed with oxo and S_P substrates, suggesting that the R_P sulfur substitution results in a smaller pK_a shift for C75. Nonetheless, similarity in the shapes and pK_a values of these three rate−pH profiles suggests that chemistry remains rate-limiting for all three substrates. The rate of the slow phase of the R_P substrate, on the other hand, did not show a dependence on pH (Figure 2C). This observation suggests that the rate of chemistry slowed to the point where another step in the mechanism has become rate-limiting (see Discussion).

Next, we quantitated the thio effects of the S_P and R_P substrates. The thio effect is the ratio of k_{obs} for the oxo and phosphorothioate substrate in the presence of Mg^{2+} (eq 3). The cleavage rate of the S_P substrate was the same as that of the oxo substrate within error at both pH 5.6 and 8.0 (Table 1)and so has no thio effect. The R_P substrate, on the other hand, displayed significant thio effects. At pH 5.6, the fast and slow phases had thio effects of ∼3- and 1000-fold, respectively, while at pH 8.0, they had thio effects of ∼5- and 800-fold, respectively (Table 1 and Figure 3A,B). (These two pH conditions were chosen to explore effects with and without protonation of C75.) In summary, sulfur substitution at the nonbridging oxygens of the scissile phosphate has a stereospecific effect, interfering with the reactivity of only the R_P substrate.

We then investigated the slow-reacting R_P phase. This phase showed pH independence and a much slower rate compared to the oxo substrate. The large thio effect observed could be a result of a large conformational change, which led us to hypothesize that the slow-reacting phase may be a result of C75 being displaced from the position observed in the WT ribozyme in this population because of the steric clash from the bulky sulfur atom at the scissile phosphate. To test this hypothesis, we conducted both biochemical and theoretical experiments.

We attempted an imidazole (0.4 M) rescue in the presence and absence of Cd^{2+} for both the R_P and oxo substrates (data not

dx.doi.org/10.1021/bi4000673 | Biochemistry 2013, 52, 6499−6514

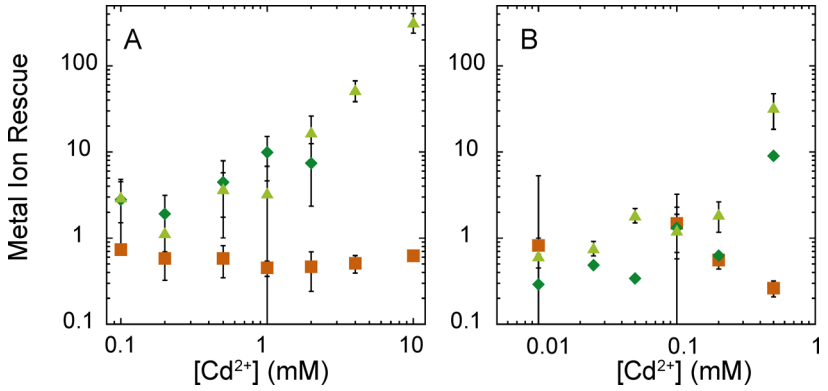

Figure 4. Metal ion rescue of the S_P and R_P substrates by Cd^{2+} ions. Metal ion rescue for the S_P (red squares), R_P fast-phase (dark green diamonds), and R_P slow-phase (light green triangles) substrates as a function of Cd^{2+} concentration at (A) pH 5.6 and (B) pH 8.0. Note that there was only a single phase for the R_P substrate at Cd^{2+} concentrations above 2 mM. Data were fit to the following version of eq 4: metal ion rescue = $(k_O/k_S)^{Mg^{2+}}/(k_O/k_S)^{Cd^{2+}}$.

shown), with the expectation of a rescue for the R_P substrate akin to those previously observed for the oxo substrate with the C75U and C75Δ mutants.[8,15] However, addition of imidazole had no effect on the reactivity of the oxo or R_P substrates (data not shown), similar to previously reported for the oxo substrate.[8] We next conducted in-line probing of the enzyme strand in the presence of 20 mM Mg^{2+} at 37 °C (Figure S3 of the Supporting Information), with the idea that if C75 is displaced within the active site, the conformation of the enzyme would be changed in some way. However, the enzyme strand did not exhibit any detectable change in cleavage pattern in the presence of the R_P substrate as compared to the oxo or S_P substrates.

In addition to biochemical studies, we conducted MD simulations on the R_P and S_P substrates bound to the HDV ribozyme. These simulations were performed in a fashion similar to that used in our previous study of the oxo substrate.[40] We found that the active site remains stable and that the various hydrogen bonds involving C75 also remain stable throughout the 25 ns MD trajectories for both the R_P and S_P substrates (Figure S4 of the Supporting Information; red, pink, and blue); the only noticeable difference between the two substrates is a small lengthening of the bond between the R_P sulfur atom and the metal ion in the R_P substrate (Figure S4A of the Supporting Information, gold) as expected. Thus, two experimental studies and one computational study provide no indication of displacement of C75 in the slowly reacting population of the R_P substrate.

Cd^{2+} Rescues the Thio Effect of the R_P Substrate. The loss of activity upon sulfur substitution at the *pro*-R_P position could be due to disruption of an interaction between a metal ion and this ligand. To test this possibility, we added thiophilic metal ions to the reaction mixture and remeasured activity, as previously described.[31,33,49−51] We studied effects of two thiophilic metal ions on the reaction kinetics, Mn^{2+} and Cd^{2+}. Addition of Mn^{2+} did not promote metal ion rescue. As shown in Table 1 and Figure S5 of the Supporting Information, addition of Mn^{2+} to a final concentration of 2 mM, in a background of 10 mM Mg^{2+} to promote native RNA folding, had no significant effect on k_{obs} for the oxo and S_P substrates and gave modest decreases in the rate of the R_P fast and slow phases of 2- and 4-fold, respectively. This led to 1.7- and 3.3-fold inverse metal ion rescues for the R_P fast and slow phases, respectively, which provides no support for a direct metal−*pro*-R_P oxygen interaction. The absence of rescue by Mn^{2+} is consistent with the earlier studies of Nishikawa and coworkers[b] on the genomic HDV ribozyme.[21]

The absence of rescue by Mn^{2+} does not, however, constitute the absence of direct metal ion−nonbridging oxygen interaction. There have been several reports that Mn^{2+} is unable to rescue the loss of reactivity upon sulfur substitution. For example, in the *Tetrahymena* group I intron, activity of the double-sulfur substitution of the *pro*-S_P oxygen and 3′-O could not be rescued by Mn^{2+} but could be rescued by Cd^{2+}.[49] We therefore measured k_{obs} in the presence of Cd^{2+}, as the concentration of Cd^{2+} was increased from 0.01 to 10 mM for pH 5.6 or from 0.01 to 0.5 mM for pH 8.0, all in a background of 10 mM Mg^{2+} to promote native RNA folding (Figure 3).[c] Increasing the concentration of Cd^{2+} decreased k_{obs} for both the oxo and S_P substrates at both low and high pH by nearly equal amounts (Figure 3A,B). This Cd^{2+}-induced inhibition of the reactivity of the oxo and S_P substrates is further revealed in plots of k_O/k_S versus Cd^{2+} concentration for S_P at low and high pH, which are essentially flat (Figure 3C,D). In contrast to the case for the oxo and S_P substrates, Cd^{2+} had essentially no effect on k_{obs} for the R_P substrate fast or slow phase (Figure 3A,B). This suggests that Cd^{2+} enhances the reactivity of the R_P substrate, thereby canceling the inhibitory effect of Cd^{2+} observed with the oxo and S_P substrates. Thus, plots of k_O/k_S versus Cd^{2+} concentration for the R_P fast and slow phases decrease with Cd^{2+} concentration at low and high pH (Figure 3C,D). This trend indicates that the impediment to ribozyme catalysis caused by the R_P sulfur substitution is assuaged to some extent by the thiophilic metal ion.

Next, we consider the magnitudes for metal ion rescue upon addition of Cd^{2+}. Metal ion rescue is calculated as $(k_O/k_S)^{Mg^{2+}}$ over $(k_O/k_S)^{Cd^{2+}}$ to correct for background effects of inhibition on the oxo substrate (eq 4). No rescue is observed for the S_P substrate with increasing concentrations of Cd^{2+} at either pH 5.6 or 8.0; indeed, metal ion rescue values stay at or slightly below unity (Figure 4). The absence of rescue by Cd^{2+} for the S_P substrate supports the absence of interaction between a metal ion and the *pro*-S_P oxygen. In contrast, metal ion rescue is present for the R_P substrate at both low and high pH and increases with Cd^{2+} concentration (Figure 4). For the slow phase, maximal Cd^{2+} rescue values of 330 ± 100 (pH 5.6) and 31 ± 9 (pH 8.0) are observed, while for the fast phase, maximal Cd^{2+} rescue values of 7.5 ± 4 (pH 5.6) and 10 ± 3 (pH 8.0) are observed (Table 1). These values are in the range of typical literature values for rescue by Cd^{2+} of 10−100-fold.[32] Overall, observation of significant metal ion rescue for the R_P fast and slow phases provides support

dx.doi.org/10.1021/bi4000673 | *Biochemistry* 2013, 52, 6499−6514

Table 2. Thio Effect in the Absence of Divalent Metal Ion, AC Double Mutant, and C75Δ Mutant

variant	pH	ionic conditions	substrate	k_{obs} (min^{-1})[a]	k_O/k_S[a]
WT without Mg^{2+}	6.0	1 M NaCl with 100 mM EDTA	oxo	$(0.5 \pm 0.1) \times 10^{-4}$	N/A[c]
			S_P	$(1.7 \pm 0.1) \times 10^{-4}$	0.3 ± 0.2
			R_P	$(0.20 \pm 0.04) \times 10^{-4}$	2.5 ± 0.3
AC DM	5.6	10 mM Mg^{2+}	oxo	0.06 ± 0.01	N/A[c]
			R_P	0.05 ± 0.01	1.1 ± 0.3
		50 mM Mg^{2+}	oxo	0.72 ± 0.01	N/A[c]
			S_P	0.57 ± 0.01	1.3 ± 0.03
			R_P	0.16 ± 0.03	4.2 ± 0.8[b]
	7.0	10 mM Mg^{2+}	oxo	0.032 ± 0.005	N/A[c]
			R_P	0.022 ± 0.002	1.5 ± 0.3
		50 mM Mg^{2+}	oxo	0.026 ± 0.001	N/A[c]
			R_P	0.018 ± 0.003	1.4 ± 0.3
C75Δ	7.0	25 mM Mg^{2+} with 400 mM imidazole	oxo	$(1.5 \pm 0.01) \times 10^{-4}$	N/A[c]
			S_P	$(2.1 \pm 0.1) \times 10^{-4}$	0.7 ± 0.03
			R_P	$(0.44 \pm 0.01) \times 10^{-4}$	3.2 ± 0.08

[a]Errors in k_{obs} and in the ratio of rate constants were determined as described in Table 1. [b]The observed thio effect could be partially (~2-fold) rescued in the presence of 0.5 mM Cd^{2+}. [c]Not applicable.

for a metal–*pro*-R_P oxygen interaction as suggested by the precleaved HDV ribozyme crystal structure.[5]

The results described above suggest that Cd^{2+} has at least two binding sites, one that is inhibitory, as revealed in the decreasing k_{obs} versus Cd^{2+} concentration plots for the oxo and S_P substrates (Figure 3A,B, blue and red bars), and one that is stimulatory, as revealed by a lack of inhibition in the presence of the R_P substrate (Figure 3A,B, dark and light green bars). (Note that if there were just a single site, then k_{obs} for the R_P substrate should increase with Cd^{2+} concentration.) The presence of inhibitory sites for Cd^{2+} with the oxo substrate is consistent with reports that Cd^{2+} inhibits the reactivity of a full-length genomic HDV ribozyme construct.[18]

We next investigated the nature of the inhibition in the oxo and S_P substrates upon Cd^{2+} addition using two different approaches. The first was an attempt to identify the binding site of the inhibitory Cd^{2+} ion. Previous Raman spectroscopic studies at pH 5.0 and 7.5 revealed a peak corresponding to a hydrated Mg^{2+} ion with at least one non-water ligand exclusively found at pH 7.5.[52] The loss of the spectral peak at low pH corresponded to the protonation of C75, because the pK_a of C75 lies within the pH range of the study, indicating that the metal ion probably lies at the active site or close to it. An inflection corresponding to a perturbation of a guanine base was also found to occur with the loss of the hydrated Mg^{2+} peak. The closest guanine residue to the active site, G1, was investigated biochemically by mutation to 7-deazaguanosine, which affected neither the Mg^{2+} requirement nor the observed rates of the reaction but did result in the loss of the spectral peak corresponding to the hydrated metal ion. Thus, this metal ion was labeled as a noncatalytic diffuse ion.[53] We investigated two mutants previously studied in the cis-acting ribozyme for their possible influence on Cd^{2+} inhibition.[54] The first mutant converts the standard G1·U37 wobble to a Watson–Crick AU base pair, while the second converts it to a G1C37 base pair. The A1U37 mutant was found herein to induce nonspecific cleavage of the two-piece system (data not shown) and was not explored further. In the case of the G1C37 mutant, we observed reactivity and found an only 3-fold decrease in the WT oxo substrate cleavage rate between 0 and 1 mM Cd^{2+} (Figure S6 of the Supporting Information). This inhibition by Cd^{2+} was weaker than that of the WT reaction (6-fold decrease), suggesting that the G1C37 mutation allows partial recovery of the inhibition by Cd^{2+}. The R_P substrate reaction was still biphasic and showed thio effects that could be rescued by Cd^{2+}, but the rescue was again not a normal rescue. Because the G1C37 mutation did not completely eliminate inhibition, the lack of a normal rescue could be due to the presence of more than one inhibitory Cd^{2+} binding site or to diffuse binding of Cd^{2+}.

In the second approach, values of k_{obs} were determined as a function of Cd^{2+} concentration at various Mg^{2+} concentrations. This was done at pH 5.6 because a wider range of Cd^{2+} concentrations could be explored without precipitation of $Cd(OH)_2$, and because C75 is protonated in a significant fraction of molecules under these conditions, which leads the active site to be more stable and less dynamic.[40] Plotting these data in the form of a Dixon plot revealed lines that intersect in the second quadrant (Figure S7 of the Supporting Information). This graphical form is consistent with inhibition by Cd^{2+} being competitive with respect to Mg^{2+}. Moreover, a value of 137 ± 73 μM for the apparent inhibition constant of Cd^{2+}, K_i, is obtained from these plots, which is significantly tighter than the apparent K_d of 16 mM observed for Mg^{2+} at pH 5.5 in the wild-type ribozyme.[11] Observation that the apparent K_i is much tighter than the apparent K_d is consistent with our recent study of the A25C20 double-mutant version of the ribozyme, wherein the catalytic metal ion appears to bind tighter than the apparent K_d for Mg^{2+}.[6] It thus appears that the inhibitory Cd^{2+} competes with the Mg^{2+} ions.

Next, we investigated the Cd^{2+} concentration dependence of rescue of the R_P substituted substrate. Interestingly, metal ion rescue by Cd^{2+} at pH 5.6 begins to assume values significantly greater than unity when the concentration of Cd^{2+} is between 1 and 2 mM (see the upwards rounding point in Figure 4A). This value is smaller than the apparent K_d of 16 mM for binding of Mg^{2+} to the oxo substrate at pH 5.5.[11] We attempted to achieve saturation of the ribozyme with Cd^{2+}; however, at Cd^{2+} concentrations higher than 10 mM, degradation of the RNA became problematic over the time scale of ribozyme cleavage (data not shown).

At pH 8.0, the metal ion rescue assumes values greater than unity when the concentration of Cd^{2+} is between 0.2 and 0.6 mM (see the upwards rounding point in Figure 4B). We are unable to saturate the reaction with Cd^{2+} ion at pH 8.0 because of the formation of cadmium hydroxide.[c] Nonetheless, rescue at lower Cd^{2+} concentrations in pH 8.0 experiments strongly suggests that

dx.doi.org/10.1021/bi4000673 | Biochemistry 2013, 52, 6499–6514

the binding of Cd^{2+} is tighter at higher pH; these trends parallel the observed pH dependence of the affinity of Mg^{2+} for the unsubstituted ribozyme.[11] Observation that the K_d for Cd^{2+}, like that of the active site Mg^{2+},[11,14] decreases with increasing pH further supports the possibility that this Cd^{2+} ion binding site is within the active site.

Role of the *pro*-R_P Oxygen in Positioning C75. The nonbridging *pro*-R_P oxygen at the scissile phosphate is positioned to interact with both the catalytic metal ion and the exocyclic amine of C75. According to the precleaved crystal structure,[5] the pro-R_P oxygen is only 2.6 Å from the metal ion but 3.6 Å from the amine of C75,[5] although MD studies in the presence of Mg^{2+} and protonated C75 indicate that this distance decreases to ~3.0 Å on average.[40] The phosphorothioate substitutions and subsequent metal ion rescues described above monitor the interaction of the nonbridging *pro*-R_P oxygen with the catalytic metal ion but do not probe its interaction with C75. In an effort to evaluate interaction between the *pro*-R_P oxygen and C75, we measured thio effects in three variant backgrounds, summarized in Table 2: (1) in 1 M NaCl and 100 mM EDTA, which removes all divalent ions, (2) in a G25·U20 to A25·C20 double mutant that interferes with active site Mg^{2+} binding, and (3) in a C75Δ mutant in which activity is rescued by imidazole. The latter two sets of experiments were conducted in the presence of Mg^{2+} ion.

We first explored whether the thio effect observed with the R_P substrate was still observable when the reaction was conducted in the absence of divalent metal ions. Although there are no divalent Mg^{2+} ions in the active site of the ribozyme under these conditions, the thio modification might interfere with any hydrogen bonding between the exocyclic amine of C75 and the scissile phosphate. The ribozyme is known to react, albeit with a reduced rate, in the absence of divalent metal ions when high concentrations of NaCl are present.[20] We employed 1 M NaCl along with 100 mM EDTA to ensure no divalent metal ion contamination. (High concentrations of EDTA are especially important because of screening from Na^+ and at low pH where EDTA binds contaminating trace divalent ions less tightly.) The R_P substrate was found to react 2.5-fold more slowly than the oxo substrate, providing a small normal thio effect (Table 2). The S_P substrate, on the other hand, reacted 3.4-fold faster than the oxo substrate, providing an inverse thio effect. Taken together, these data provide no clear support for the *pro*-R_P oxygen interacting directly with C75, or any other functionality.

Next, we investigated the effect of phosphorothioate substitution on the reaction with the A25·C20 double mutant. The reverse G·U wobble found at the active site contributes to the electronegative pocket for the divalent metal ion.[5,6,42] Mutating this reverse wobble to an isosteric A·C reverse wobble replaces the keto oxygen of guanine with the amine of the adenine. This A25·C20 double mutant has been reported to have a bell-shaped rate−pH profile for the ribozyme in the presence of added divalent metal ions, with pK_a values of 5.4 ± 0.3 and 6.2 ± 0.2.[6] This rate−pH profile is largely an inverse of the trend observed in the WT ribozyme and suggests that any contribution of the catalytic metal ion to the reaction with the A·C reverse wobble occurs only at low pH. According to the crystal structure of the precleaved ribozyme with a reverse G·U wobble, the *pro*-R_P oxygen interacts directly with the catalytic metal ion and with the exocyclic amine on C75 (Figure 1B). In the absence of any contribution from the catalytic metal ion, as anticipated for the A25·C20 double mutant at neutral pH, we expected to exclusively interrogate the interaction of the *pro*-R_P oxygen with the exocyclic amine on C75.

When we analyzed the reaction of this double mutant with the thio substrates, no thio effect was observed for the R_P substrate at neutral pH in 10 or 50 mM Mg^{2+} [thio effects of 1.5 ± 0.3 and 1.4 ± 0.3, respectively (Table 2)], consistent with absence of strong metal binding in the active site of the A25·C20 double mutant at biological pH as previously concluded.[6] Importantly, these data further provide no direct support for the *pro*-R_P oxygen interacting with C75, as a thio effect should have been observed in the absence of divalent metal ion if this were the case. It is possible, however, that this interaction is present but that it is redundant with other interactions at the active site (see Discussion).

At the lower pH of 5.6, no thio effect was observed for the R_P substrate in the A·C double mutant in 10 mM Mg^{2+} (Table 2), again providing no support for the *pro*-R_P oxygen interacting with C75. However, at pH 5.6 and the elevated Mg^{2+} concentration of 50 mM, a 4.2 ± 0.8-fold thio effect was observed for the R_P substrate (Table 2). This effect was stereospecific in that it was absent with the S_P substrate, which gave a 1.3 ± 0.03-fold effect (Table 2). These data suggest that only at the lowest pH, where C75 is protonated and the active site is aligned[40] and at the highest Mg^{2+} concentrations can the A·C double mutant support the direct metal ion interaction at the active site. Consistent with this notion, we observed a partial rescue of this thio effect by Cd^{2+} (Table 2, footnote). These data further support direct *pro*-R_P oxygen−Mg^{2+} interaction at the active site and are also consistent with the upward arm observed in the rate−pH profile for the A·C double mutant between pH 5 and 5.5 at 50 mM Mg^{2+}.[6]

Lastly, we measure the effect of phosphorothioate substitution in the C75Δ background. These experiments were conducted in the presence of 25 mM Mg^{2+} and 0.4 M imidazole, which are optimal for folding and C75 rescue under these conditions.[10] First, we note that all three substrates were cleaved in the presence of the C75Δ enzyme. A 3.2 ± 0.08-fold thio effect was observed for the R_P substrate that was absent with the S_P substrate, which exhibited a 0.7 ± 0.03-fold effect (Table 2). These data further support the importance of interaction between the *pro*-R_P oxygen and the catalytic metal ion, even in the absence of the amine of C75. This also suggests that any interaction between the *pro*-R_P oxygen and C75 is relatively unimportant for *pro*-R_P oxygen function with metal ion. In summary, the thio effects observed in 1 M NaCl and 100 mM EDTA, the A·C double mutant, and C75Δ further support the direct *pro*-R_P oxygen−Mg^{2+} interaction but provide no clear support for direct interaction between the *pro*-R_P oxygen and N4 of C75 or any other functionality in the reaction.

QM/MM Study of the Thio Effect at the Scissile Phosphate. To investigate the effect of phosphorothioate substitution at the scissile phosphate theoretically, we performed geometry optimizations on the phosphorothioate-substituted R_P and S_P substrates in the presence of the catalytic Mg^{2+} ion. The optimized reactant structure of the R_P substrate exhibited significant active site distortion (Figure 5A) compared to the optimized reactant structure of the oxo species. The most prominent effect was the increase in the distance between C75(N3) and G1(O5′) by ~0.7 Å. These two atoms serve as the donor and acceptor, respectively, for the proton transfer reaction that is a key step in the self-cleavage reaction of the ribozyme.[27] Moreover, the distance between the catalytic ion and the *pro*-R_P sulfur increased by ~0.5 Å compared to that distance in the oxo species. These two distortions are consistent with the significantly slower rates of the R_P substrate observed experimentally in the presence of Mg^{2+}. In contrast, no such

dx.doi.org/10.1021/bi4000673 | *Biochemistry* 2013, 52, 6499−6514

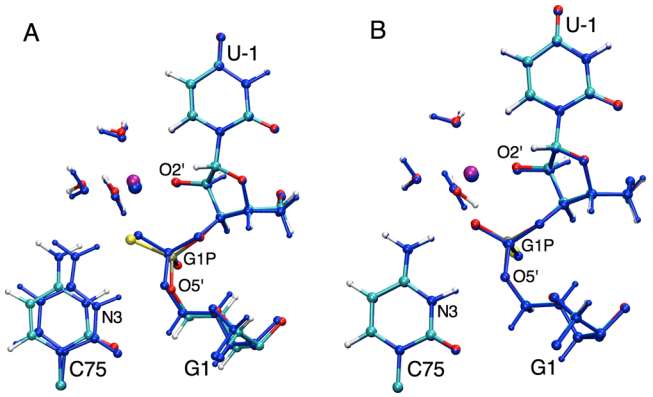

Figure 5. Overlay of the cleavage site of the QM/MM-optimized reactant states for WT oxo with S_P and R_P substrates with Mg^{2+} ion at the catalytic site. Overlays of (A) oxo and R_P substrates and (B) oxo and S_P substrates. The phosphorothioate-containing structures are colored cyan and atom-specific colors, with the catalytic Mg^{2+} ion colored purple. The WT structure and its catalytic Mg^{2+} ion are colored entirely blue. In all three structures, N3 of C75 is protonated.

distortions were observed in the optimized reactant state of the S_P substrate (Figure 5B).

For the R_P substrate, we identified a transition state (TS) using the quasi-synchronous transit method and performed frequency calculations to confirm that the resulting stationary point has a single imaginary frequency (Figure 6). This transition state has a structure similar to that of the reactant structure, except for the position of the proton (H3) on N3(C75), which has partially transferred to O5′(G1). Starting from this TS structure, we calculated the mass-weighted minimum energy path (MEP) back to the reactant and product structures following the intrinsic reaction coordinate (IRC) (Figure 6A,B). When we followed this path in the product direction, we obtained a minimum corresponding to an intermediate in which the proton has fully transferred to G1(O5′) (Figure 6C). The calculated energy barriers along this pathway are 37 and 5 kcal/mol in the forward and reverse directions, respectively. While these energies cannot be used to calculate reaction rate constants because they do not include entropic effects and represent only one possible reaction pathway, they can still be used to gain qualitative insight into the mechanism. This reaction path suggests that the reaction mechanism is sequential, with the proton transferring prior to phosphorus−oxygen bond formation and cleavage. In contrast, prior analogous QM/MM calculations on the oxo species suggested a concerted mechanism with a phosphorane-like transition state when a divalent ion is bound at the catalytic site.[27] Moreover, the calculated energy barrier from the reactant to the TS is 12 kcal/mol higher for the R_P substrate than for the oxo substrate, although the energetics are not reliable because of the incomplete sampling of conformational space.[27] We emphasize that the search for transition states was not fully comprehensive, and other transition states with different character may also exist.

Although this sequential reaction pathway with initial proton transfer does not seem probable based on the high energy barrier, we propose a possible explanation for why it may be followed by the R_P substrate. The *pro*-R_P oxygen of the scissile phosphate interacts with both the catalytic metal ion and the exocyclic amine of C75. Replacing this oxygen with sulfur weakens both of these interactions. The weakening of the *pro*-R_P−N4(C75) interaction causes C75 to move away from G1, thus increasing the proton donor−acceptor distance from 3.01 Å in WT to 3.72 Å in the R_P substrate for the optimized reactant state. Note that the proton donor−acceptor distance decreases to 2.75 Å at the transition state of the first step depicted in Figure 6 for the R_P substrate to allow proton transfer. An explanation for why the proton may be transferred in the first step of a sequential mechanism for the R_P substrate is that the weakening of the *pro*-R_P−metal ion interaction may strengthen the metal ion−O2′(U−1) interaction, thereby hindering the attack of the O2′ nucleophile on the scissile phosphate.

QM/MM Study of the Metal Ion Rescue by Cd^{2+} at the Scissile Phosphate. To understand the role of Cd^{2+} ion in rescuing the catalytic reaction, we performed QM/MM calculations after replacing the catalytic Mg^{2+} ion with a Cd^{2+}

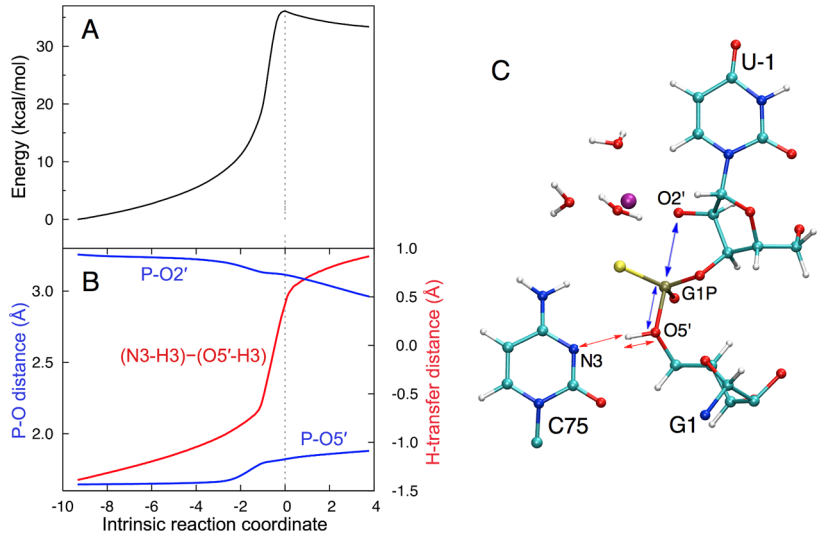

Figure 6. Minimum energy path (MEP) obtained from the QM/MM calculations for the initial proton transfer step of the self-cleavage reaction catalyzed by the R_P substrate with Mg^{2+} ion at the catalytic site. This step corresponds to the transfer of a proton from N3(C75) to O5′(G1) and would be followed by a step comprised of phosphorus−oxygen bond formation and cleavage. (A) Energy and (B) relevant distances shown along the intrinsic reaction coordinate. (C) Scissile phosphate region of the intermediate corresponding to a proton transferred from N3(C75) to O5′(G1), which is the product of the MEP for the step shown in panels A and B. Colors on arrows are coordinated with colors in panel B.

dx.doi.org/10.1021/bi4000673 | *Biochemistry* 2013, 52, 6499−6514

ion. For both the oxo and S_P substrates in the presence of Cd^{2+}, we were unable to identify a transition state or intermediate associated with either a concerted or a sequential mechanism. Several constrained optimization techniques were utilized to search for both a phosphorane intermediate and an intermediate corresponding to initial proton transfer. Although these searches were not comprehensive, the calculations suggest that the oxo and S_P substrate species behave similarly (i.e., with no stable intermediates) when Cd^{2+} is bound at the active site. In the actual experiment, Mg^{2+} is also present and presumably binds at the active site and drives the reaction for the oxo and S_P substrates. For the R_P substrate, the data support Cd^{2+} binding at the active site and participating in the reaction.

For the R_P substrate in the presence of Cd^{2+}, we tried to locate an intermediate similar to the one observed for the R_P substrate with a Mg^{2+} ion at the catalytic site [i.e., with the proton transferred to O5′(G1)] using several constrained optimization techniques but were unsuccessful. However, we were able to locate a phosphorane intermediate as a minimum on the potential energy surface (Figure 7). Formation of a phosphorane

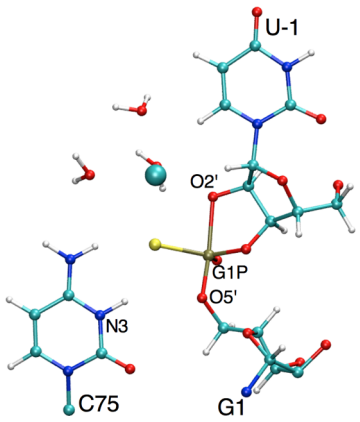

Figure 7. Cleavage site of the phosphorane intermediate structure obtained from the QM/MM calculations for the R_P substrate with Cd^{2+} ion at the catalytic site.

intermediate species has been shown to be involved in similar ribozyme-catalyzed reactions.[55] Moreover, in our previous study,[27] we reported a phosphorane intermediate for the oxo case with a monovalent ion (Li^+, Na^+, K^+, or Cs^+) at the catalytic site, in contrast to the concerted reaction pathway observed with a divalent ion at the catalytic site (Mg^{2+} or Ca^{2+}). The absence of an intermediate arising from initial proton transfer for the R_P substrate in the presence of Cd^{2+} can be attributed to the strengthening of the Cd^{2+}–*pro*-R_P sulfur interaction and the weakening of the Cd^{2+}–O2′(U−1) interaction, thereby allowing the O2′ nucleophile to attack the scissile phosphate to form the phosphorane intermediate structure.

For the R_P substrate, the type of intermediate observed depends on the particular metal ion at the active site. In terms of energetics, the intermediate corresponding to proton transfer identified in the presence of Mg^{2+} was 33 kcal/mol higher than the optimized reactant, whereas the phosphorane intermediate identified in the presence of Cd^{2+} was only 10 kcal/mol higher than the optimized reactant. Although these values are not quantitatively meaningful, the large difference is consistent with the experimental observation that the overall reaction of the R_P substrate is more facile in the presence of Cd^{2+}.

DISCUSSION

The importance of nucleobase and metal ion catalysis in ribozyme mechanism has been established, but the extent of cooperation between them remains unclear. A recent crystal structure of the precleaved genomic HDV ribozyme indicated interaction between the catalytic metal ion and the *pro*-R_P oxygen of the scissile phosphate,[5] but previous functional studies did not provide evidence that supported this interaction.[21] Herein, we utilized experimental and theoretical methods to assess the functional importance of the *pro*-R_P oxygen at the active site. The R_P sulfur substitution at the scissile phosphate resulted in biphasic kinetics with a thio effect as large as ∼1000 that could be rescued with the thiophilic metal ion Cd^{2+}. These data, in contrast to previously reported results, implicate the *pro*-R_P oxygen of the scissile phosphate as a catalytically important metal ion ligand. Furthermore, QM/MM calculations support the importance of the *pro*-R_P oxygen and help explain the experimentally observed thio effects for the R_P substrate. Interaction between the *pro*-R_P oxygen and C75 was also investigated via experiments conducted in the absence of bound divalent metal ion. These studies provided no normal thio effect and thus no clear evidence of catalytically important interaction between the exocyclic amine of C75 and the *pro*-R_P oxygen, although the absence of a large normal thio effect cannot be equated to an absence of interaction.

Comparison to Other Studies of the HDV Ribozyme Using Phosphorothioate Substitutions. The *pro*-R_P oxygen on the scissile phosphate of the HDV ribozyme has been studied previously in both the genomic and antigenomic versions of the HDV ribozyme. At present, crystal structures are available only for the genomic ribozyme, in both cleaved and precleaved states.[3,5,56] The previous study of phosphorothioate modifications on the genomic version of the ribozyme was conducted in the presence of 10 mM Mg^{2+} by Nishikawa and co-workers.[21] They reported nearly identical behavior for the S_P and oxo substrates, similar to our findings (Table 1). They also reported that the R_P substrate reacted to only ∼10−20% completion and that this phase had no thio effect, which is similar although not identical to our findings. We too found that ∼30% R_P substrate reacted in a fast phase, although this phase has a modest thio effect of ∼5-fold at pH 8.0. These differences can perhaps be attributed to our construct being rate-limited by chemistry and therefore faster-reacting. We note that those authors did not include time points longer than 30 min; the slow phase in our reaction has $t_{1/2}$ values of ∼175 and ∼75 min at pH 5.6 and 8.0, respectively (Table 1), long enough that the previous study may have missed this phase in their slower-reacting constructs. Moreover, the previous experiments attempted rescue only in 10 mM Mn^{2+}, a mildly thiophilic metal ion,[31] and did not find any rescue.[21] This observation is similar to that herein in 10 mM Mg^{2+} and 2 mM Mn^{2+}, although we see slight inverse metal ion rescues (Table 1).

In the antigenomic version of the ribozyme, phosphorothioate substitution of the *pro*-R_P oxygen was reported to give a significant 25-fold thio effect that was partially (4-fold) rescued by either 1 mM Cd^{2+} or 1 mM Mn^{2+}, both in the background of 9 mM Mg^{2+}.[57] The authors thus concluded that the *pro*-R_P oxygen participates in a metal ion interaction. These data support a direct interaction of the catalytic metal with the *pro*-R_P oxygen in the antigenomic ribozyme, similar to that found herein for the genomic ribozyme. Although no crystal structure currently exists for the antigenomic ribozyme, the two ribozymes are closely related and their active site nucleotides are strongly conserved across evolution.[58,59] Also, the thio effects for the R_P substrate of

dx.doi.org/10.1021/bi4000673 | *Biochemistry* 2013, 52, 6499−6514

~25-fold in the antigenomic and ~5-fold (fast phase) in the genomic ribozymes are significant but relatively small (see the last section of Discussion), consistent with our previous study that concluded that divalent metal ion contributes only ~25-fold to catalysis.[12] The large thio effect of ~1000-fold for the slow phase of the R_P substrate may be due to a change to a different reaction pathway, as supported by flattening of the rate−pH profile.

In the study of phosphorothioate effects in the antigenomic HDV ribozyme, several mutations near the active site were also examined for thio effects and metal ion rescue.[57] These led to reduced thio effects and small or inverse metal ion rescues. These mutants largely reacted slower than the wild type with the natural oxo substrate. This illustrates that slowly reacting ribozymes can lead to a loss of thio effects, most likely when the rate-limiting step is not chemistry. This phenomenon may account for why Nishikawa and co-workers did not observe a thio effect on the R_P substrate for the genomic ribozyme.[21]

Support for a Metal Ion Interacting Directly with the Scissile Phosphate. The observation of a large stereospecific thio effect indicates the importance of the *pro*-R_P oxygen for the reaction but does not itself establish direct interaction between the metal ion and the *pro*-R_P oxygen. For this purpose, metal ion rescue with a thiophilic metal ion such as Cd^{2+} was conducted. Metal ion rescue generally supports direct metal ion−ligand interaction and is defined mathematically as $(k_O/k_S)^{Mg^{2+}}$ divided by $(k_O/k_S)^{Cd^{2+}}$. Typically, for a metal ion rescue in the presence of Cd^{2+}, k_S increases while k_O does not change. However, in the study presented here, k_S did not change while k_O decreased. In other words, the metal ion rescue observed herein is unconventional in that it is complicated by an inhibitory effect of Cd^{2+} on the WT oxo substrate (Figure S7 of the Supporting Information) and a lack of stimulation of the R_P substrate (Figure 3A).

The observation described above can be ascribed to one of several limiting scenarios. In scenario 1, a single Cd^{2+} ion interacts with the S_P and oxo substrates at the active site but not the R_P substrate. In this case, the Cd^{2+} would inhibit the S_P and oxo substrates but somehow be displaced by the *pro*-R_P sulfur atom. Although this scenario cannot be ruled out, it seems unlikely for two reasons. First, we analyzed all of the known metal ion binding sites in the precleaved crystal structure. For those sites near the active site, none has interaction with an N7 as would be expected for a transition metal binding site. Second, all Cd^{2+} experiments were performed in a background of 10 mM Mg^{2+}. Because the active site is characterized with an extensive presence of phosphate nonbridging oxygens, the Mg^{2+} is expected to interact with these much more strongly than the Cd^{2+}.

In scenario 2, a single Cd^{2+} ion interacts with and inhibits the oxo, S_P, and R_P substrates but not at the scissile phosphate; at the same time, a second Cd^{2+} ion interacts specifically with the R_P substrate at the scissile phosphate and stimulates the reaction. The model of a common inhibitory site is supported by the mutational data at the cleavage site base pair presented in the Results: interaction of metal ion with N7 of G1 was suggested by prior comparison of divalent and monovalent ions from theoretical and experimental methods as well as analysis of the known metal ion binding sites.[53] Indeed, Cd^{2+} inhibited the G1C37 mutant less than the wild type (Figure S6 of the Supporting Information; 3- and 6-fold inhibition, respectively), suggesting that at least a portion of the Cd^{2+} inhibition comes from this site. In further support of scenario 2, inspection of the structure suggests several other distal sites that could contribute to inhibition. Moreover, Nishikawa and co-workers found that Cd^{2+} fully inhibits the wild-type genomic ribozyme but only partially inhibits a version in which the last 5 bp and the loop of P4 were replaced with UUU, which supports Cd^{2+} inhibition originating, at least in part, from the genome-specific P4 region of the ribozyme.[18] Additionally, similar inhibition by Cd^{2+} was found in the RNase P ribozyme with increasing Cd^{2+} concentration.[60] Their phosphorothioate experiments were unable to determine either the nature of the inhibition or the number of inhibitory metal binding sites, but the relative rate of the unmodified to the thio substitution at the cleavage site was found to be rescued with the addition of Cd^{2+}, similar to results found in our study.

Lastly, we note that the affinities of the inhibitory and stimulatory Cd^{2+} ions for their respective sites should be similar; otherwise, the rate of the R_P substrate should be faster (or slower) for Cd^{2+} concentrations between the two dissociation constants, and a bell-shaped curve would result, which was not observed (Figure 3A). Observation of an upwards rounding point near 1 mM for the dependence of metal ion rescue on Cd^{2+} concentration (Figure 4A) is consistent with studies of Ward and DeRose, who measured a $K_{1/2}$ for binding of Cd^{2+} to the R_P substrate in the hammerhead ribozyme of 900 μM in 15 mM Ca^{2+} and 100 mM Na^+,[61] an ionic strength background somewhat similar to that of 10 mM Mg^{2+} and 50 mM Na^+ used herein.

Theoretical calculations herein revealed different mechanisms for the oxo and R_P substrates in the presence of Mg^{2+} as well as the R_P substrate in the presence of Cd^{2+}. The mechanism previously identified for the oxo species in the presence of Mg^{2+} is concerted with a phosphorane-like transition state,[27] while the mechanism identified for the R_P substrate in the presence of Mg^{2+} has an intermediate arising from proton transfer with a very high energy barrier (Figure 6). The observation of a high-energy intermediate for the R_P substrate in the QM/MM calculations is consistent with the thio effect observed experimentally. The calculations suggested another mechanism for cleavage of the R_P substrates in the presence of Cd^{2+}, namely a sequential mechanism with a phosphorane intermediate. For the R_P substrate, the energy of the optimized intermediate relative to the optimized reactant is ~23 kcal/mol lower in the presence of Cd^{2+} than in the presence of Mg^{2+}. This observation is consistent with the experimentally observed thiophilic metal ion rescue. The inhibitory effect observed in the case of the oxo and S_P substrates in the presence of Cd^{2+} could not be explained by the theoretical model. The lack of knowledge about the various possible metal binding sites for the metal ion makes it difficult to address this issue through theoretical calculations.

The *pro*-R_P Oxygen Is Not Necessary for Positioning C75. Experiments conducted in the absence of Mg^{2+} ions in 1 M NaCl and 100 mM EDTA showed either a small normal thio effect, with the R_P substrate, or a small inverse thio effect, with the S_P substrate. In an effort to understand the inverse thio effect, we considered the charge distribution on the nonbridging O and S atoms from experimental and theoretical viewpoints. Frey and Sammons discussed that crystals of thiophosphate diester monoanions display similar bond orders for the P−S and P−O bonds and thus likely have similar charge distributions on the nonbridging O and S.[62] We calculated Mulliken and CHELPG charges[63,64] with the sulfur atom at the nonbridging position and also found that negative charge was approximately evenly distributed between the nonbridging O and S atoms (data not shown). In addition, theoretical calculations on phosphate diesters from York and co-workers indicated that although sulfur may be more polarizable and thus capable of inducing charge

dx.doi.org/10.1021/bi4000673 | *Biochemistry* 2013, 52, 6499−6514

localization, the large sulfur atom tends to be less well solvated, again leading to a nearly even charge distribution on the two nonbridging atoms.[65,66] Thus, the inverse thio effect does not appear to be due to uneven charge distribution between the nonbridging O and S atoms.

It is interesting to note that an inverse thio effect in monovalent ions has been previously observed for both the genomic and antigenomic ribozymes.[20] In the presence of NaCl, the genomic ribozyme gave rise to a 3.3-fold inverse thio effect for the S_P substrate,[d] identical to that seen herein (Table 2), while in the presence of NH_4Cl, very large inverse thio effects of 18- and 34-fold were observed for the genomic and antigenomic ribozymes, respectively, for the S_P substrate. These authors pointed to a possible change in the active site geometry with the thiophosphate. At present, the origin of the inverse thio effect remains unclear. Nonetheless, our experiments in the absence of divalent ions provide no clear support for a direct interaction between the exocyclic amine on C75 and the *pro*-R_P oxygen atom, although they do not rule it out either (see also below).

Experiments with the A·C double mutant showed lack of a thio effect in all but the low-pH, high-metal ion conditions. These observations strongly support the conclusion that the *pro*-R_P oxygen is not necessary for positioning C75. Lastly, experiments with C75Δ indicated that any interaction between the *pro*-R_P oxygen and C75 is not critical for *pro*-R_P–metal ion interaction.

These observations raise the question of what interactions are important for positioning C75 for the transfer of a proton to the leaving group. In the crystal structure, the *pro*-R_P oxygen of C22 forms a 3.0 Å hydrogen bond with N4 of C75,[5] and MD studies in the presence of Mg^{2+} and protonated C75 indicate an average distance of ∼2.8 Å.[40] This distance is somewhat shorter than the distance between N4 of C75 and the *pro*-R_P oxygen at the scissile phosphate in both the crystal structure and MD, suggesting that the phosphate of C22 might be relatively more important in the positioning of C75. In addition, C75 is positioned by a hydrogen bond between O5′ of G1 and N3 of C75 found in both the crystal structure and MD (Figure 1B), and C75 forms a strong stacking interaction with A77. This multitude of interactions involving C75 may make any one contact redundant to its positioning. Such principles have been applied to nonadditivity in enzymology.[67] Indeed, we have argued for low cooperativity of RNA folding in a tetraloop hairpin, where the multitude of stacking, hydrogen bonding, and hydration interactions provides an extensive and overdetermined network of interactions that make any single interaction nonessential.[68,69] Thus, the lack of significant contributions of the scissile phosphate *pro*-R_P oxygen in interacting with C75 observed herein does not mean that these two species do not interact.

The R_P Substrate Has Biphasic Kinetics. The studies described here used a two-piece ribozyme construct, which facilitated introduction of the phosphorothioate at the cleavage site and separation of the diastereomers. We studied the oxo, S_P, and R_P substrates with the same enzyme strand. The oxo and S_P substrates gave simple, single-exponential kinetic behavior, as reflected in the traces in Figure 2. The R_P substrate, however, gave double-exponential kinetics under most conditions despite using the same enzyme strand as for the other substrates. The origin of the biphasic behavior is not entirely clear, although simple results with the oxo and S_P substrates suggest that it is unlikely due to problems with heterogeneity in the ribozyme strand, which has beset other ribozymes.[70]

The fast and slow phases of the R_P substrate have quite different behavior. The thio effects are only up to ∼5-fold for the fast phase but up to ∼1000-fold for the slow phase. Observation of thio effects is consistent with the theoretical studies in which the R_P substrate was observed to follow a reaction pathway with a high-energy proton transfer intermediate (Figure 6). However, the QM/MM calculations presented here cannot speak to the biphasic nature of the R_P substrate kinetics. Moreover, metal ion rescue is 7.5- and 330-fold for the fast and slow phases, respectively. Thus, in general, larger thio effects and metal ion rescues are found for the slower phase. In addition, the R_P substrate fast phase showed a typical rate–pH profile, albeit with a slightly lower pK_a than the oxo and S_P substrates (Figure 2B), while the slow phase did not show a dependence on pH (Figure 2C). This large thio effect does not appear to be due to displacement of C75 on the basis of the absence of imidazole rescue of the R_P substrate, the absence of significant refolding as per in-line probing assays, and the lack of C75 extrusion in MD trajectories (see Results). Thus, this large thio effect may be due to a change in the reaction pathway, and further studies will be needed to elucidate it.

Comparison to Studies of Other Ribozymes Using Phosphorothioate Substitutions. In the opening section of the Discussion, we compared our results with those from previous studies of the HDV genomic and antigenomic ribozymes that used phosphorothioate substitutions. Having identified similarities and differences among these studies, we provide here a brief comparison between phosphorothioate studies on the HDV ribozymes and several other ribozymes. We compare thio effects, metal ion specificity, and then metal ion rescues.

Metal ion rescue studies have been employed extensively on the *Tetrahymena* group I[31,32,49,71] and hammerhead[61,72–74] ribozymes to investigate the nature and the extent of interactions between their catalytic metal ions and their potential ligands. The *Tetrahymena* ribozyme is a metalloenzyme that uses two or three metal ions in its catalytic mechanism.[71,75] It is a well-understood and absolutely divalent metal ion-dependent ribozyme. Magnitudes of thio effects in the *Tetrahymena* ribozyme, which occur for both *pro*-R_P and *pro*-S_P oxygens, range from several-fold to 1200-fold. These values span a range similar to that of the thio effects we observe for the *pro*-R_P oxygen herein: up to 5-fold for the fast phase and 1000-fold for the slow phase.

The identity of the metal used in metal ion rescue experiments is critical in the *Tetrahymena* ribozyme. Metal ion rescues for the *Tetrahymena* ribozyme were often specific to one particular thiophilic metal ion, such as Mn^{2+}, Zn^{2+}, or Cd^{2+}, and depended on the ion–ligand pair that was being studied.[32,51,71] This likely arises because metal–ligand interactions can be exquisitely sensitive to the ligand geometry. In the HDV ribozyme, we also observe that metal ion rescues are specific to particular thiophilic metal ions, for instance Cd^{2+} but not Mn^{2+} rescues in the genomic ribozyme. Also, the magnitude of the metal ion rescues in the HDV ribozyme are similar to those in the group I ribozyme, with values for the R_P substrate of 7.5-fold for the fast phase and 330-fold for the slow phase, similar to the values of 5–330-fold found for the group I ribozyme.

Earlier phosphorothioate rescue experiments with the hammerhead ribozyme focused on the minimal ribozyme, which lacks key tertiary contacts as compared to the full-length ribozyme.[76] Thio effects on the order of >10,000-fold were found to be specific to the R_P substrate.[72] Interestingly, thio effects on the full-length hammerhead ribozyme are only ∼100-fold for the R_P substrate.[61] The lack of extensive tertiary contacts in the minimal ribozyme may result in a larger conformational change

dx.doi.org/10.1021/bi4000673 | *Biochemistry* 2013, 52, 6499–6514

upon the introduction of the bulky sulfur atom at the scissile phosphate leading to larger thio effects. In addition, the smaller thio effect in the full-length hammerhead ribozyme is consistent with the small ~25-fold contribution of metal ions to catalysis,[77,78] qualitatively similar to the studies herein. Metal ion rescue for the R_P substrate of the full-length hammerhead ribozyme is ~9-fold, similar to the rescue observed for the fast phase in the studies described here. Overall, the observation that thio effects and metal ion rescues for the HDV ribozyme are quantitatively and qualitatively similar to those of the *Tetrahymena* and the hammerhead ribozymes supports a critical role for metal ions in the active site of the HDV ribozyme.

■ ASSOCIATED CONTENT

Supporting Information

Data on the HPLC separation of the thio substrates, iodine cleavage, ILP, MD simulations of the thio substrates with the enzyme strand, metal ion rescue with Mn^{2+}, and inhibition of the oxo substrate by Cd^{2+}. This material is available free of charge via the Internet at http://pubs.acs.org.

■ AUTHOR INFORMATION

Corresponding Author

*B.L.G.: e-mail, barbgolden@purdue.edu; telephone, (765) 496-6165; fax, (765) 494-7897. S.H.-S.: e-mail, shs3@illinois.edu; telephone, (217) 300-0335. P.C.B.: e-mail, pcb5@psu.edu; telephone, (814) 863-3812; fax, (814) 865-2927.

Funding

This work was supported by National Institutes of Health (NIH) Grant R01GM095923 to B.L.G. and P.C.B. and NIH Grant GM056207 to S.H.-S.

Notes

The authors declare no competing financial interest.

■ ACKNOWLEDGMENTS

We thank Squire Booker and Tyler Grove for use of their HPLC instrument for the separation of the phosphorothioate diastereomers, Ji Chen for providing the clone for the A25·C20 double-mutant ribozyme, and Andrew Sirjoosingh for help with Figure S7. We also thank Vickie DeRose, Joe Piccirilli, and Mike Harris for insightful discussions.

■ ABBREVIATIONS

HDV, hepatitis delta virus; QM/MM, quantum mechanical/molecular mechanical; R_P/S_P substrate, substrate strand with a sulfur substitution at the nonbridging *pro*-R_P/S_P oxygen on the scissile phosphate; MEP, minimum energy path; WT, wild type.

■ ADDITIONAL NOTES

[a]The slightly lower value may be due to experiments herein being on a two-piece construct and the referenced pK_a being on a one-piece construct. Recent pK_a values on the two-piece construct at 5 mM Mg^{2+} were lower than those on the one-piece construct by 0.3 pK_a unit.[6]

[b]These studies did not reveal the decrease in R_P rate with Mn^{2+}, but they used more Mn^{2+}, without Mg^{2+}, and employed a slower-reacting ribozyme. Nonetheless, there is overall agreement about the inability of Mn^{2+} to rescue the reaction.

[c]$K_{S_P}[Cd(OH)_2] = 5.9 \times 10^{-15}$ at 37 °C, and at pH 8.0 $[OH^-]$ ~2.5×10^{-6} M, using a K_w of ~2.5×10^{-14} at 37 °C. For $Cd(OH)_2$ to be soluble at pH 8.0, $Q = [Cd^{2+}][OH^-]^2 < 5.9 \times 10^{-15}$. Thus, the Cd^{2+} concentration was kept at <1 mM at pH 8.0.

[d]The diastereomers were left as a mixture in that study, but the authors provided evidence that the more reactive portion comes from the S_P substrate.

■ REFERENCES

(1) Lai, M. M. C. (1995) The molecular biology of hepatitis delta virus. *Annu. Rev. Biochem. 64*, 259−286.

(2) Tseng, C.-H., and Lai, M. M. C. (2009) Hepatitis delta virus RNA replication. *Viruses 1*, 818−831.

(3) Ferré-D'Amaré, A. R., Zhou, K., and Doudna, J. A. (1998) Crystal structure of a hepatitis delta virus ribozyme. *Nature 395*, 567−574.

(4) Perrotta, A. T., and Been, M. D. (1991) A pseduknot-like structure required for efficient self-cleavage of the hepatitis delta virus RNA. *Nature 350*, 434−436.

(5) Chen, J.-H., Yajima, R., Chadalavada, D. M., Chase, E., Bevilacqua, P. C., and Golden, B. L. (2010) A 1.9 Å crystal structure of the HDV ribozyme precleavage suggests both Lewis acid and general acid mechanisms contribute to phosphodiester cleavage. *Biochemistry 49*, 6508−6518.

(6) Chen, J., Ganguly, A., Miswan, Z., Bevilacqua, P. C., Hammes-Schiffer, S., and Golden, B. L. (2013) Identification of the catalytic Mg^{2+} ion in the HDV ribozyme. *Biochemistry 52*, 557−567.

(7) Golden, B. L. (2011) Two distinct catalytic strategies in the hepatitis δ virus ribozyme cleavage reaction. *Biochemistry 50*, 9424−9433.

(8) Perrotta, A. T., Shih, I., and Been, M. D. (1999) Imidazole rescue of a cytosine mutation in a self-cleaving ribozyme. *Science 286*, 123−126.

(9) Shih, I. H., and Been, M. D. (2001) Involvement of a cytosine side chain in proton transfer in the rate-determining step of ribozyme self-cleavage. *Proc. Natl. Acad. Sci. U.S.A. 98*, 1489−1494.

(10) Perrotta, A. T., Wadkins, T. S., and Been, M. D. (2006) Chemical rescue, multiple ionizable groups, and general acid-base catalysis in the HDV genomic ribozyme. *RNA 12*, 1282−1291.

(11) Nakano, S., Chadalavada, D. M., and Bevilacqua, P. C. (2000) General acid-base catalysis in the mechanism of a hepatitis delta virus ribozyme. *Science 287*, 1493−1497.

(12) Nakano, S., Proctor, D. J., and Bevilacqua, P. C. (2001) Mechanistic characterization of the HDV genomic ribozyme: Assessing the catalytic and structural contributions of divalent metal ions within a multichannel reaction mechanism. *Biochemistry 40*, 12022−12038.

(13) Nakano, S., and Bevilacqua, P. C. (2007) Mechanistic characterization of the HDV genomic ribozyme: A mutant of the C41 motif provides insight into the positioning and thermodynamic linkage of metal ions and protons. *Biochemistry 46*, 3001−3012.

(14) Gong, B., Chen, J.-H., Chase, E., Chadalavada, D. M., Yajima, R., Golden, B. L., Bevilacqua, P. C., and Carey, P. R. (2007) Direct measurement of a pK_a near neutrality for the catalytic cytosine in the genomic HDV ribozyme using Raman crystallography. *J. Am. Chem. Soc. 129*, 13335−13342.

(15) Das, S. R., and Piccirilli, J. A. (2005) General acid catalysis by the hepatitis delta virus ribozyme. *Nat. Chem. Biol. 1*, 45−52.

(16) Draper, D. E. (2004) A guide to ions and RNA structure. *RNA 10*, 335−343.

(17) Fedor, M. J., and Williamson, J. R. (2005) The catalytic diversity of RNAs. *Nat. Rev. Mol. Cell Biol. 6*, 399−412.

(18) Suh, Y. A., Kumar, P. K., Taira, K., and Nishikawa, S. (1993) Self-cleavage activity of the genomic HDV ribozyme in the presence of various divalent metal ions. *Nucleic Acids Res. 21*, 3277−3280.

(19) Nakano, S., Cerrone, A. L., and Bevilacqua, P. C. (2003) Mechanistic characterization of the HDV genomic ribozyme: Classifying the catalytic and structural metal ion sites within a multichannel reaction mechanism. *Biochemistry 42*, 2982−2994.

(20) Perrotta, A. T., and Been, M. D. (2006) HDV ribozyme activity in monovalent cations. *Biochemistry 45*, 11357−11365.

(21) Fauzi, H., Kawakami, J., Nishikawa, F., and Nishikawa, S. (1997) Analysis of the cleavage reaction of a trans-acting human hepatitis delta virus ribozyme. *Nucleic Acids Res. 25*, 3124−3130.

(22) Jeoung, Y. H., Kumar, P. K., Suh, Y. A., Taira, K., and Nishikawa, S. (1994) Identification of phosphate oxygens that are important for self-cleavage activity of the HDV ribozyme by phosphorothioate substitution interference analysis. *Nucleic Acids Res. 22*, 3722−3727.
(23) Chadalavada, D. M., Knudsen, S. M., Nakano, S., and Bevilacqua, P. C. (2000) A role for upstream RNA structure in facilitating the catalytic fold of the genomic hepatitis delta virus ribozyme. *J. Mol. Biol. 301*, 349−367.
(24) Gong, B., Chen, Y., Christian, E. L., Chen, J.-H., Chase, E., Chadalavada, D. M., Yajima, R., Golden, B. L., Bevilacqua, P. C., and Carey, P. R. (2008) Detection of innersphere interactions between magnesium hydrate and the phosphate backbone of the HDV ribozyme using Raman crystallography. *J. Am. Chem. Soc. 130*, 9670−9672.
(25) Nakano, S., and Bevilacqua, P. C. (2001) Proton inventory of the genomic HDV ribozyme in Mg^{2+}-containing solutions. *J. Am. Chem. Soc. 123*, 11333−11334.
(26) Cerrone-Szakal, A. L., Siegfried, N. A., and Bevilacqua, P. C. (2008) Mechanistic characterization of the HDV genomic ribozyme: Solvent isotope effects and proton inventories in the absence of divalent metal ions support C75 as the general acid. *J. Am. Chem. Soc. 130*, 14504−14520.
(27) Ganguly, A., Bevilacqua, P. C., and Hammes-Schiffer, S. (2011) Quantum mechanical/molecular mechanical study of the HDV ribozyme: Impact of the catalytic metal ion on the mechanism. *J. Phys. Chem. Lett. 2*, 2906−2911.
(28) Gish, G., and Eckstein, F. (1988) DNA and RNA sequence determination based on phosphorothioate chemistry. *Science 240*, 1520−1522.
(29) Suydam, I. T., and Strobel, S. A. (2009) Nucleotide analog interference mapping. *Methods Enzymol. 468*, 3−30.
(30) Soukup, G. A., and Breaker, R. R. (1999) Relationship between internucleotide linkage geometry and the stability of RNA. *RNA 5*, 1308−1325.
(31) Herschlag, D., Piccirilli, J. A., and Cech, T. R. (1991) Ribozyme-catalyzed and nonenzymatic reactions of phosphate diesters: Rate effects upon substitution of sulfur for a nonbridging phosphoryl oxygen atom. *Biochemistry 30*, 4844−4854.
(32) Frederiksen, J. K., and Piccirilli, J. A. (2009) Identification of catalytic metal ion ligands in ribozymes. *Methods 49*, 148−166.
(33) Szewczak, A. A., Kosek, A. B., Piccirilli, J. A., and Strobel, S. A. (2002) Identification of an active site ligand for a group I ribozyme catalytic metal ion. *Biochemistry 41*, 2516−2525.
(34) Bevington, P. R. (1969) *Data reduction and error analysis for the physical sciences*, McGraw-Hill, New York.
(35) Segel, I. H. (2003) *Enzyme kinetics*, Wiley, New York.
(36) Bowers, K. J., Chow, E., Xu, H., Dror, R. O., Eastwood, M. P., Gregersen, B. A., Klepeis, J. L., Kolossvary, I. K., Moraes, M. A., Sacerdoti, F. D., Salmon, J. K., Shan, Y., and Shaw, D. E. (2006) Proceedings of the ACM/IEEE Conference on Supercomputing (SC06).
(37) *Desmond Molecular Dynamics System* (2008) D. E. Shaw Research, New York.
(38) Cornell, W. D., Cieplak, P., Bayly, C. I., Gould, I. R., Merz, K. M., Ferguson, D. M., Spellmeyer, D. C., Fox, T., Caldwell, J. W., and Kollman, P. A. (1995) A second generation force field for the simulation of proteins, nucleic acids, and organic molecules. *J. Am. Chem. Soc. 117*, 5179−5197.
(39) Wang, J., Cieplak, P., and Kollman, P. A. (2000) How well does a restrained electrostatic potential (RESP) model perform in calculating conformational energies of organic and biological molecules? *J. Comput. Chem. 21*, 1049−1074.
(40) Veeraraghavan, N., Ganguly, A., Golden, B. L., Bevilacqua, P. C., and Hammes-Schiffer, S. (2011) Mechanistic strategies in the HDV ribozyme: Chelated and diffuse metal ion interactions and active site protonation. *J. Phys. Chem. B 115*, 8346−8357.
(41) Veeraraghavan, N., Bevilacqua, P. C., and Hammes-Schiffer, S. (2010) Long-distance communication in the HDV ribozyme: Insights from molecular dynamics and experiments. *J. Mol. Biol. 402*, 278−291.
(42) Veeraraghavan, N., Ganguly, A., Chen, J.-H., Bevilacqua, P. C., Hammes-Schiffer, S., and Golden, B. L. (2011) Metal binding motif in the active site of the HDV ribozyme binds divalent and monovalent ions. *Biochemistry 50*, 2672−2682.
(43) *DESMOND* (2009) D. E. Shaw Research, New York.
(44) *Qsite* (2008) Schrodinger, LLC, New York.
(45) Becke, A. D. (1993) A new mixing of Hartree−Fock and local density-functional theories. *J. Chem. Phys. 98*, 1372−1377.
(46) Cramer, C. J. (2002) *Computational chemistry*, Chapters 5−8.
(47) Hehre, W. J. (2003) *A guide to molecular mechanics and quantum mechanical calculations*, Chapter 2.
(48) Kaminski, G. A., Friesner, R. A., Tirado-Rives, J., and Jorgensen, W. L. (2001) Evaluation and reparametrization of the OPLS-AA force field for proteins via comparison with accurate quantum chemical calculations on peptides. *J. Phys. Chem. B 105*, 6474−6487.
(49) Yoshida, A., Sun, S., and Piccirilli, J. A. (1999) A new metal ion interaction in the *Tetrahymena* ribozyme reaction revealed by double sulfur substitution. *Nat. Struct. Biol. 6*, 318−321.
(50) Hamm, M. L., Nikolic, D., Van Breemen, R. B., and Piccirilli, J. A. (2000) Unconventional origin of metal ion rescue in the hammerhead ribozyme reaction: Mn^{2+}-assisted redox conversion of 2′-mercaptocytidine to cytidine. *J. Am. Chem. Soc. 122*, 12069−12078.
(51) Shan, S., Kravchuk, A. V., Piccirilli, J. A., and Herschlag, D. (2001) Defining the catalytic metal ion interactions in the *Tetrahymena* ribozyme reaction. *Biochemistry 40*, 5161−5171.
(52) Chen, J.-H., Gong, B., Bevilacqua, P. C., Carey, P. R., and Golden, B. L. (2009) A catalytic metal ion interacts with the cleavage site G·U wobble in the HDV ribozyme. *Biochemistry 48*, 1498−507.
(53) Golden, B. L., Hammes-Schiffer, S., Carey, P. R., and Bevilacqua, P. C. (2013) An integrated picture of HDV ribozyme catalysis. In *Biophysics of RNA Folding*, pp 135−168, Springer, New York.
(54) Cerrone-Szakal, A. L., Chadalavada, D. M., Golden, B. L., and Bevilacqua, P. C. (2008) Mechanistic characterization of the HDV genomic ribozyme: The cleavage site base pair plays a structural role in facilitating catalysis. *RNA 1*, 1746−1760.
(55) Wei, K., Liu, L., Cheng, Y.-H., Fu, Y., and Guo, Q.-X. (2007) Theoretical examination of two opposite mechanisms proposed for hepatitis delta virus ribozyme. *J. Phys. Chem. B 111*, 1514−1516.
(56) Ke, A., Zhou, K., Ding, F., Cate, J. H., and Doudna, J. A. (2004) A conformational switch controls hepatitis delta virus ribozyme catalysis. *Nature 429*, 201−205.
(57) Wrzesinski, J., Wichłacz, A., Nijakowska, D., Rebowska, B., Nawrot, B., and Ciesiołka, J. (2010) Phosphate residues of antigenomic HDV ribozyme important for catalysis that are revealed by phosphorothioate modification. *New J. Chem. 34*, 1018−1026.
(58) Rosenstein, S. P., and Been, M. D. (1991) Evidence that genomic and antigenomic RNA self-cleaving elements from hepatitis delta virus have similar secondary structures. *Nucleic Acids Res. 19*, 5409−5416.
(59) Wadkins, T. S., Perrotta, A. T., Ferré-D'Amaré, A. R., Doudna, J. A., and Been, M. D. (1999) A nested double pseudoknot is required for self-cleavage activity of both the genomic and antigenomic hepatitis delta virus ribozymes. *RNA 5*, 720−727.
(60) Sun, L., and Harris, M. E. (2007) Evidence that binding of C5 protein to P RNA enhances ribozyme catalysis by influencing active site metal ion affinity. *RNA 13*, 1505−1515.
(61) Ward, W. L., and Derose, V. J. (2012) Ground-state coordination of a catalytic metal to the scissile phosphate of a tertiary-stabilized hammerhead ribozyme. *RNA 18*, 16−23.
(62) Frey, P. A., and Sammons, D. (1985) Bond order and charge localization in nucleoside phosphorothioates. *Science 228*, 541−545.
(63) Mulliken, R. S. (1955) Electronic population analysis on LCAO MO molecular wave functions. *J. Chem. Phys. 23*, 1833−1840.
(64) Breneman, C. M., and Wiberg, K. B. (1990) Determining atom-centered monopoles from molecular electrostatic potentials. The need for high sampling density in formamide conformational analysis. *J. Comput. Chem. 11*, 361−373.
(65) Liu, Y., Lopez, X., and York, D. M. (2005) Kinetic isotope effects on thio-substituted biological phosphoryl transfer reactions from density-functional theory. *Chem. Commun. 31*, 3909−3911.
(66) Liu, Y., Gregersen, B. A., Hengge, A., and York, D. M. (2006) Transesterification thio effects of phosphate diesters: Free energy

barriers and kinetic and equilibrium isotope effects from density-functional theory. *Biochemistry 45*, 10043−10053.
(67) Kraut, D. A., Carroll, K. S., and Herschlag, D. (2003) Challenges in enzyme mechanism and energetics. *Annu. Rev. Biochem. 72*, 517−571.
(68) Moody, E. M., Feerrar, J. C., and Bevilacqua, P. C. (2004) Evidence that folding of an RNA tetraloop hairpin is less cooperative than its DNA counterpart. *Biochemistry 43*, 7992−7998.
(69) Siegfried, N. A., and Bevilacqua, P. C. (2009) Thinking inside the box: Designing, implementing, and interpreting thermodynamic cycles to dissect cooperativity in RNA and DNA folding. *Methods Enzymol. 455*, 365−393.
(70) Greenfeld, M., Solomatin, S. V., and Herschlag, D. (2011) Removal of covalent heterogeneity reveals simple folding behavior for P4-P6 RNA. *J. Biol. Chem. 286*, 19872−19879.
(71) Forconi, M., Lee, J., Lee, J. K., Piccirilli, J. A., and Herschlag, D. (2008) Functional identification of ligands for a catalytic metal ion in group I introns. *Biochemistry 47*, 6883−6894.
(72) Scott, E. C., and Uhlenbeck, O. C. (1999) A re-investigation of the thio effect at the hammerhead cleavage site. *Nucleic Acids Res. 27*, 479−484.
(73) Maderia, M., Hunsicker, L. M., and Derose, V. J. (2000) Metal-phosphate interactions in the hammerhead ribozyme observed by ^{31}P NMR and phosphorothioate substitutions. *Biochemistry 39*, 12113−12120.
(74) Suzumura, K., Takagi, Y., Orita, M., and Taira, K. (2004) NMR-based reappraisal of the coordination of a metal ion at the pro-R_P oxygen of the A9/G10.1 site in a hammerhead ribozyme. *J. Am. Chem. Soc. 126*, 15504−15511.
(75) Stahley, M. R., and Strobel, S. A. (2005) Structural evidence for a two-metal-ion mechanism of group I intron splicing. *Science 309*, 1587−1590.
(76) Blount, K. F., and Uhlenbeck, O. C. (2005) The structure-function dilemma of the hammerhead ribozyme. *Annu. Rev. Biophys. Biomol. Struct. 34*, 415−440.
(77) O'Rear, J. L., Wang, S., Feig, A. L., Beigelman, L., Uhlenbeck, O. C., and Herschlag, D. (2001) Comparison of the hammerhead cleavage reactions stimulated by monovalent and divalent cations. *RNA 7*, 537−545.
(78) Curtis, E. A., and Bartel, D. P. (2001) The hammerhead cleavage reaction in monovalent cations. *RNA 7*, 546−552.
(79) Brown, T. S., Chadalavada, D. M., and Bevilacqua, P. C. (2004) Design of a highly reactive HDV ribozyme sequence uncovers facilitation of RNA folding by alternative pairings and physiological ionic strength. *J. Mol. Biol. 341*, 695−712.